Dissertation

submitted to the

Combined Faculty of Mathematics, Engineering and Natural Sciences

of the Ruprecht - Karls - University Heidelberg

obtaining the doctoral degree of

Doctor of Natural Science

Presented by

Shruthi Hemanna, M.Sc.

Born in: Bangalore, India

Oral Examination: 3rd May 2024

Targeting EEF1A in fibroblasts to counteract cardiac fibrosis

Referees: Prof. Dr. Thomas Wieland

Prof. Dr. Jörg Heineke

Acknowledgement

I am writing to express sincere gratitude to everyone who has played a significant role in completing this dissertation. I am deeply thankful to Jörg Heineke for his support, guidance, and valuable insights throughout my research journey. His expertise and encouragement were instrumental in shaping this dissertation.

I extend my gratitude to Prof. Thomas Wieland for his valuable feedback and constructive suggestions throughout my doctoral studies as faculty supervisor for the Bioscience faculty of Heidelberg. Additionally, I would like to thank Professor Dr. Marc Freichel and Dr. Chi-Chung Wu for accepting to be the Doctoral Defense committee examiners.

I want to thank Abel for sharing his expertise and teaching techniques, which contributed to developing my research skills and helped me grow as a scientist. A huge thanks to Nina and Merve, who have strengthened my journey during this doctoral study. They have constantly supported me throughout the challenges of these academic years. I will forever cherish their friendship. I am grateful to every lab member from AG Heineke, namely Aya, Steve, Rhys, Ekaterina, and Amelie, for their support, brainstorming for every lab-related problem and for giving me some beautiful memories, and to AG Dieterich, especially Lothar, Alperen, Emma, and Pragati for their unwavering support and motivation, especially during my thesis writing time.

I want to thank Mannheim's Medical faculty and Heidelberg's Bioscience faculty for providing me with an honorable platform and granting me the doctoral degree.

I would be remiss if I did not mention my family and friends, especially my Dad- Hemanna, my sister Shilpa, and most importantly, my niece Dhriti for their motivation, prayers, patience,

and unconditional love, which kept me going through the roller coaster rides life through at me. A special thanks to Ingrid, who has been a constant source of positive energy and her good wishes and my go-to person for any situation.

Finally, I would like to Thank God and my mom, who has guided me through all the hurdles and helped me finish this degree.

I miss you, Mom.

Contents

Abbreviations

AD	Adenovirus
AMcFB	Adult mouse cardiac fibroblast
ATF4	Activating transcription factor 4
ATF6	Activating transcription factor 6
ATP	Adenosine triphosphate
BCA	Bicinchoninic acid assay
BiP	Binding immunoglobulin protein
BL6	Black 6
BrdU	Bromodeoxyuridine
BSA	Bovine serum albumin
CAD	Coronary Artery Disease
CHD	Coronary heart disease
CHOP,	C/EBP homologous protein
CO_2	Carbon di-oxide
Col1a1	Collagen, type I, alpha 1
Col3a1	Collagen, type 3, alpha 1
CVD	Cardiovascular Diseases
DAPI	4',6-diamidino-2-phenylindole
DMEM	Dulbecco's Modified Eagle Medium
DNA	Deoxyribonucleic acid
ECL	Enhanced chemiluminescence
ECM	extracellular matrix
EEF	Eukaryotic elongation factor
EEF1A	Eukaryotic elongation factor 1 alpha
EEF1A1	Eukaryotic elongation factor 1 alpha 1
EEF1A2	Eukaryotic elongation factor 1 alpha 2
EF1B,	Elongation factor 1 beta
EF2	elongation factor 2
EF-TU	elongation factor thermo unstable
EIF2AK3	eukaryotic translation initiation factor 2 alpha kinases
ELISA	enzyme-linked immunosorbent assay
EMBL	European Molecular biology laboratory
EMBO	European Molecular Biology Organization
ER	Endoplasmic reticulum
ESC	Embryonic stem cells
FB	Fibroblasts
FCS	Fetal bovine serum
FN1	Fibronectin 1
GAPDH	glyceraldehyde-3-phosphate dehydrogenase
GDP	Guanosine diphosphate
GEF	Guanine nucleotide exchange factors

GTP	Guanosine-5'-triphosphate
HCL	Hydrochloric acid
HEK	Human embryonic kidney
HF	Heart Failure
HRP	Horseradish peroxidase
HSP70	Heat shock protein 70
IF2	Initiation factor 2
IRE1	Inositol-requiring enzyme type 1
KD	Knockdown
KDEL	amino acid sequence
LC3b	microtubule-associated protein light chain 3 beta
LIMA	Live cell imaging Mannheim
M199	Medium 199
MAPK	Mitogen-activated protein Kinases
MEF	Mouse embryonic fibroblast
MMPs	matrix metalloproteinases
MOI	Multiplicity of infection
mTOR1	mammalian target of rapamycin complex 1
NAFLD	Nonalcoholic fatty liver disease
NASH	Nonalcoholic steatohepatitis
NF-κB	nuclear factor kappa B
NRcFB	Neonatal cardiac fibroblast
NTP	Nucleoside triphosphate
PAD	Peripheral artery disease
PBS	Phosphate-buffered saline
PCNA	Proliferating cell nuclear antigen
PCR	Polymerase chain reaction
PE	phosphatidylethanolamine
PERK	PKR-like endoplasmic reticulum kinase
PFA	Paraformaldehyde
PFU	Plaque-forming unit
PKB-(Akt1)	Protein Kinase B
PUMA	p53 upregulated modulator of apoptosis
PVDF	Polyvinylidene difluoride
RIPA	Radioimmunoprecipitation assay
RNA	Ribonucleic acid
RSV	respiratory syncytial virus
RT	Reverse transcription
SDS	Sodium dodecyl sulfate
SEM	Standard error of Mean
SM22	Smooth muscle protein 22
SMA	Smooth muscle actin
SMAD	Suppressor of Mothers against Decapentaplegic
SQSTM1	Sequestosome 1

SUnSET	Surface sensing of translation
TBST	Tris-Buffered Saline with 0.1% Tween 20
TGFβ	Transforming growth factor beta
TIMPs	tissue inhibitor of metalloproteinases
UPR	Unfolded protein response
WT	Wildtype
ZPR1	zinc finger protein 1

List of Tables

List of Figures

Abstract

Background: Despite recent advancements, heart failure remains the leading cause of death in the Western world. Since fibrosis is a central and deleterious feature of cardiac remodelling leading to heart failure, there is a great interest in identifying new targets that can ameliorate or even reverse cardiac fibrosis. The canonical role of the eukaryotic elongation factor 1 alpha (eEF1A) is to deliver aa-tRNAs to the ribosome; in addition, it holds non-canonical functions in regulating autophagy, aggresome formation, and proteasome activity.

Methods and Results: This study aimed to investigate the potential role of eEF1A in promoting pro-fibrotic activity in fibroblasts. Fibroblasts express mainly eEF1A1 and only minimal amounts of the eEF1A2 isoform. Mouse embryonic fibroblasts (MEF) were isolated from eEF1A1/A2 flox/flox mice and incubated with either a control (Adβgal) or a Cre-recombinase expressing adenovirus (Ad. Cre). A strong downregulation (>70%) of total eEF1A both at the mRNA and protein levels, which was followed by a significant downregulation of fibrosis-associated genes, such as Col1a1, αSMA, Col3a1, FN, and Sm22 at the mRNA as well as at the protein level (Col1a1, αSMA) was observed. As expected, global protein synthesis activity (assessed with the SUnSET assay) was downregulated by around 50% in MEFs with downregulation of eEF1A (eEF1A-KD). A harringtonine run-off assay indicated a reduced translational elongation speed in the KD cells. These findings of a considerable downregulation of extracellular matrix proteins (αSMA, SM22, FN, Col1a1, and Col3a1) were confirmed upon approximately 50% downregulation of eEF1A in adult cardiac fibroblasts (AMcFB) by quantitative analysis using Western blot and RT-qPCR. Next, various cellular-based assays were performed to assess the effect of eEF1A on the functional properties of fibroblasts (MEF), and observed a significant decrease in proliferation and migration capacity

after eEF1A knock-down (KD) was observed. Investigations into autophagy in eEF1A-KD cells (MEF) revealed an upregulation in p62 (by +50%) and LC3b (by +500%) compared to control cells. Given the crucial role of ER stress in maintaining proteostasis and this study's finding of an upregulation of the unfolded protein response (UPR) following eEF1A knockdown, the UPR could rescue proteostasis under these circumstances. Therefore, this study suggests that further in-depth analysis is essential to elucidate the underlying mechanism and the adaptive responses triggered by the downregulation of eEF1A in fibroblasts.

Conclusions: Counteracting eEF1A expression reduces general protein synthesis and triggers autophagy in fibroblasts, while predominantly reducing pro-fibrotic activity in these cells in vitro. Therefore, targeting eEF1A by specific inhibitors could be an anti-fibrotic therapeutic strategy in the future.

Zusammenfassung

Hintergrund: Trotz der jüngsten Fortschritte bleibt die Herzinsuffizienz die häufigste Todesursache in der westlichen Welt. Da Herzfibrose ein zentrales und schädliches Element der Herzinsuffizienz ist, ist die Identifikation neuer Zielproteine, die die Herzfibrose lindern oder sogar umkehren können, von großem Interesse. Die kanonische Funktion des eukaryotischen Elongationsfaktors 1 alpha (eEF1A) besteht darin, aa-tRNAs an das Ribosom zu bringen; darüber hinaus hat er weitere Funktionen bei der Regulation von Autophagie, Aggresombildung und der Proteasom-Aktivität.

Methoden und Ergebnisse: Ziel dieser Studie war es, die mögliche Rolle von eEF1A in der pro-fibrotischen Aktivität von Fibroblasten zu untersuchen. Fibroblasten exprimieren hauptsächlich eEF1A1 und nur geringe Mengen der eEF1A2-Isoform. Embryonale Mausfibroblasten (MEF) wurden aus eEF1A1/A2 flox/flox Mäusen isoliert und entweder mit einem Kontrollvirus (Adβgal) oder einem Cre-Rekombinase exprimierenden Adenovirus (Ad. Cre) inkubiert. Dadurch wurde eine starke Herunterregulierung (>70%) des gesamten eEF1A sowohl auf der mRNA- als auch auf der Proteinebene erzielt, gefolgt von einer signifikanten Herabregulierung von Fibrose-assoziierten Genen wie Col1a1, αSMA, Col3a1, FN und Sm22 auf der mRNA- als auch auf der Proteinebene (Col1a1, αSMA). Wie erwartet, wurde die globale Proteinsyntheseaktivität (gemessen mit dem SUnSET-Assay) um etwa 50 % in MEFs mit herunterreguliertem eEF1A (eEF1A-KD) reduziert. Per Harringtonin-Ablauf Assay wurde eine verringerte Translationsgeschwindigkeit in den KD-Zellen detektiert. Diese Befunde einer beträchtlichen Herabregulierung der extrazellulären Matrixproteine (αSMA, SM22, FN, Col1a1 und Col3a1) wurden auch in adulten mäusen kardialen Fibroblasten (AMkFB) bei einer etwa

ca. 50%igen Reduktion von eEF1A mittels Western Blot und RT-qPCR bestätigt. Anschließend wurden verschiedene zellbasierte Tests durchgeführt, um die Auswirkungen von eEF1A auf die Funktion von Fibroblasten (MEF) zu bewerten. Eine signifikante Abnahme der Proliferations- und Migrationskapazität nach eEF1A-Knockdown (KD) wurde beobachtet. Untersuchungen zur Autophagie in eEF1A-KD-Zellen (MEF) zeigten eine Hochregulierung von p62 (um +50%) und LC3b (um +500%) im Vergleich zu Kontrollzellen. Angesichts der entscheidenden Rolle von ER-Stress bei der Aufrechterhaltung der Proteostase und der in dieser Studie festgestellten Hochregulierung der „Unfolded Protein Response" (UPR) nach dem Knockdown von eEF1A, könnte die UPR unter diesen Umständen die Proteostase nach eIEF2A-Reduktion stabilisieren.

Daher sind weitere eingehende Analysen erforderlich, um den zugrunde liegenden Mechanismus und die adaptiven Reaktionen, die durch die Reduktion von eEF1A in Fibroblasten ausgelöst werden, aufzuklären.

Schlussfolgerungen: Die Hemmung der eEF1A-Expression reduziert die allgemeine Proteinsynthese und löst Autophagie in Fibroblasten aus, während die fibrotische Aktivität dieser Zellen in vitro abnimmt. Daher könnte die Reduktion von eEF1A durch spezifische Inhibitoren einen neuartige, antifibrotischen Therapieansatz in der Zukunft darstellen.

1. Introduction

1.1. Cardiovascular Diseases

Cardiovascular diseases (CVD) have been a global health concern, contributing to the highest non-cancer disease related cause for mortality[1]. Cardiovascular system comprises of the heart and blood vessels which naturally gives rise to the foundation of many clinical conditions which can be encompassed in four entities: Coronary Artery Disease (CAD),Cerebrovascular disease, Peripheral artery disease (PAD), aortic atherosclerosis [2]. Aortic atherosclerosis is commonly caused by abdominal aortic aneurism. Peripheral artery disease is developed due to plaque formation in the peripheral arteries narrowing the pathway of blood flow from the heart to other parts of the body. Cerebrovascular disease is a condition caused due to an acute compromise of cerebral perfusion or vasculature leading to the ischemic strokes. Coronary artery diseases also known as coronary heart diseases (CHD) has been the majority percentage of cause of CVD related death. CAD/CHD are sustained due to reduced myocardial perfusion upon persistence anginal discomfort eventually resulting in myocardial infarction and/or heart failure [2].

1.2. Heart Failure

Heart failure (HF) has been a major global concern due to its high rate of mortality. The ages and clinical signs associated with HF can vary from different ethnicities and regions in the world population. Asians tend to show the symptoms of early HF between 35 to 45 years of age compared to Europeans and other Western countries [3].

Heart failure is characterized as a clinical syndrome resulting from the organ's incompetence, involving both structural and/or functional aspects to match the necessary volume of blood and oxygen supply to be matched with sufficient metabolic demands[4, 5]. HF can develop over time, manifested as multiple major clinical symptoms in patients. The symptoms may also be evident in single organ level or multiple organ malfunctions. For example, chronic heart failure can accompanied by acute lung damage or liver cirrhosis[4].

According to the American Heart College of Cardiology, there has been studies conducted to decipher different stages of HF and their corresponding risk factors. One major risk factor which develops into HF is hypertension, diabetes mellitus, and a family history of cardiomyopathy. The second most common stage is asymptomatic HF which is described as previous caused myocardial infarction, left ventricular dysfunctions, valvular heart disease. The third stage is symptomatic HF during physical exercise, structural heart disease, dyspnea [4]. All of these stages can be encompassed within a section developing cardiovascular disease, which has been a growing concern in medical field for its progressive attribution to morbidity and mortality.

1.3. Myocardial Remodeling

The heart is one of the most complex organs of mammalian species, which remodels itself in response to various stimuli and stressors. Remodeling can be termed a change of physical size and shape due to structural alterations. Evidence shows that all cardiac remodeling does not necessarily lead to heart malfunctions and sometimes can be adaptive and compensated for improving the cardiovascular system[6, 7].

Remodeling involves inducing pressure on the intraventricular myofibrils, and can also serve as a compensatory mechanism in case of pressure/volume overload leading to hypertrophy and ventricular dilatation to improve the cardiac pumping output. The myocardium functions with homogeneously of the different cardiac cell types with their respective functions. When the equilibrium of the cardiac function is imbalanced due to the mechanical stress and stimuli, which then leads to the heterogeneity of the non- cardiomyocyte's population in the tissue. This, in turn, triggers pathological remodeling, which leads to the structural and ultrastructural aberrations and pushes the heart tissue to undergo compensatory repairs[8]. These repairs and remodeling lead to increased deposition of extracellular matrix proteins, mainly collagen, differentiation into myofibroblast, hypertrophy of the myocytes, and removal of necrotic cardiomyocytes (Figure 1). Importantly, these compensatory measures can also help preserve the cardiac function before allowing the compensatory mechanism to become detrimental[6, 9]. The aberration of the cardiac functions and myocardium remodeling depends on the duration of heart failure; the longer the heart failure symptoms persist in patients, the stronger the fibrosis[9].

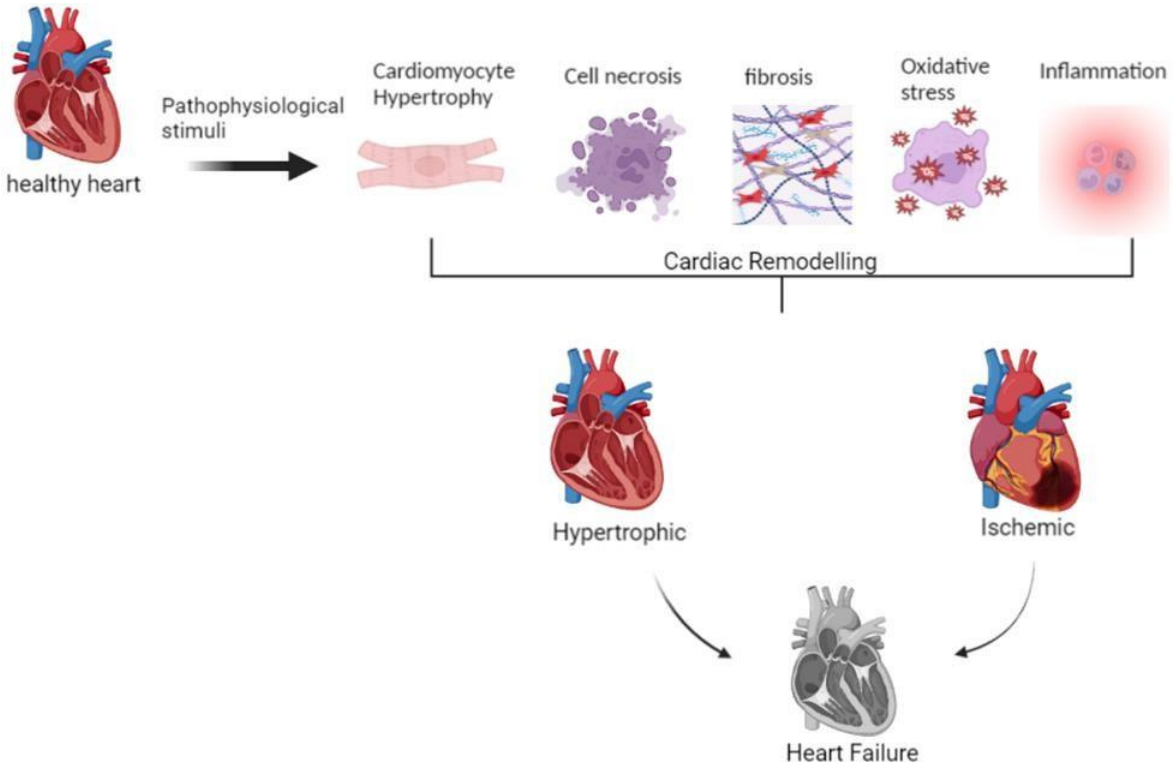

Figure 1: Scheme showing cardiac remodeling.
Due to Pathophysiological stimuli in heart, different cell type undergoes pathological changes contributing to cardiac remodeling leading to hypertrophic or ischemic condition, which upon induced stressed dilates the myocardium resulting in heart failure. Illustration done using biorender.com

1.4. Cardiac Fibrosis

Heart tissue scarring and abnormal thickening can result in various cardiac diseases and cardio-malfunctions, collectively known as cardiac fibrosis. These prolonged cardiac conditions may result in poor prognosis and heart failure[10]. Hence, some cardiac fibrosis conditions could be reversed by early detection with specific management. However, when detected in advanced stages, the treatment options are limited and the condition can be irreversible, so the entire focus is shifted to handling and treating the symptoms, maximizing the ability to increase life span[10, 11].

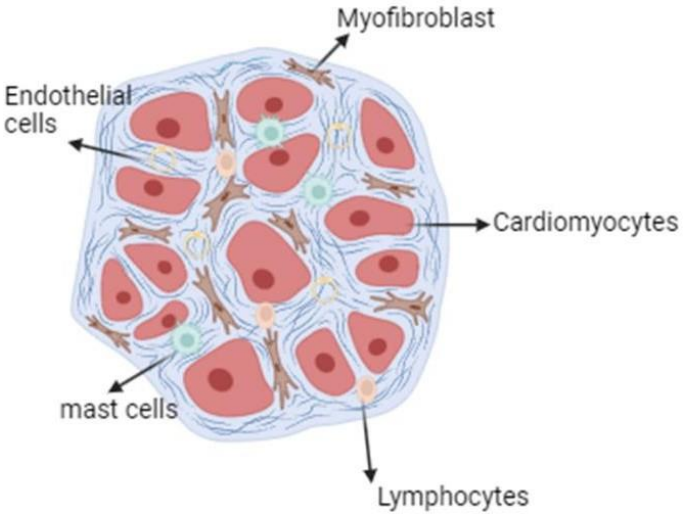

Figure 2: Pictorial representation of fibrotic heart tissue with the cell types.
Graphical representation of hypertrophy cardiomyocytes, upon stimulation from cytokines or cells-like mast, endothelial leads to fibroblasts differentiate into myofibroblast. *Illustration done using biorender.com*

Cardiac fibrosis can be characterized into many types and defined as under an umbrella of excessive accumulation of the matrix proteins upon inflammatory response[11]. Heart tissue, mainly adult, is not a regenerative tissue; therefore, the myocardium shows massive death of cardiomyocytes due to acute myocardial infarction[12]. Aging could also contribute to the progression of cardiac fibrosis, leading to diastolic heart failure in aged patients. Hypertrophy is another major factor contributing to the remodeling of the myocardium due to sustained pressure/ volume overload, which can be accompanied by severe fibrosis with dilation of the ventricles resulting in systolic heart failure[10].

Fibroblast is one of the primary cell types of the myocardium apart from cardiomyocytes and endothelial cells. The ratio of these three major cell types in terms of population generally depends upon gender, age, and species. During fibrosis, main source of collagens has been

directed from activated fibroblast also known as myofibroblasts, induced by the production of pro-inflammatory cytokines, angiogenic factors [11, 13, 14] (shown as pictorial representation in Figure 2). Based on recent fibrosis studies, the contribution of fibroblasts is known to be the primary effector cell type that alters the structure of the myocardium, as its main function is to maintain the integrity of homeostasis within cellular remodeling [11, 14, 15].

1.5. Proteostasis

Proteostasis is a cellular process that involves the maintenance of the cellular and system homeostasis, including the life-cycle of proteins starting from synthesis to its degradation. Any alteration caused in this course of these interconnecting pathways can lead to irreparable damage being a cause for some well-known diseases such as Alzheimer's, diabetes, cancer, and heart failure. The cellular process involves different functions such as synthesis of new proteins, misfolding or degradation, transporting the synthesized or misguided proteins to its target site [16].

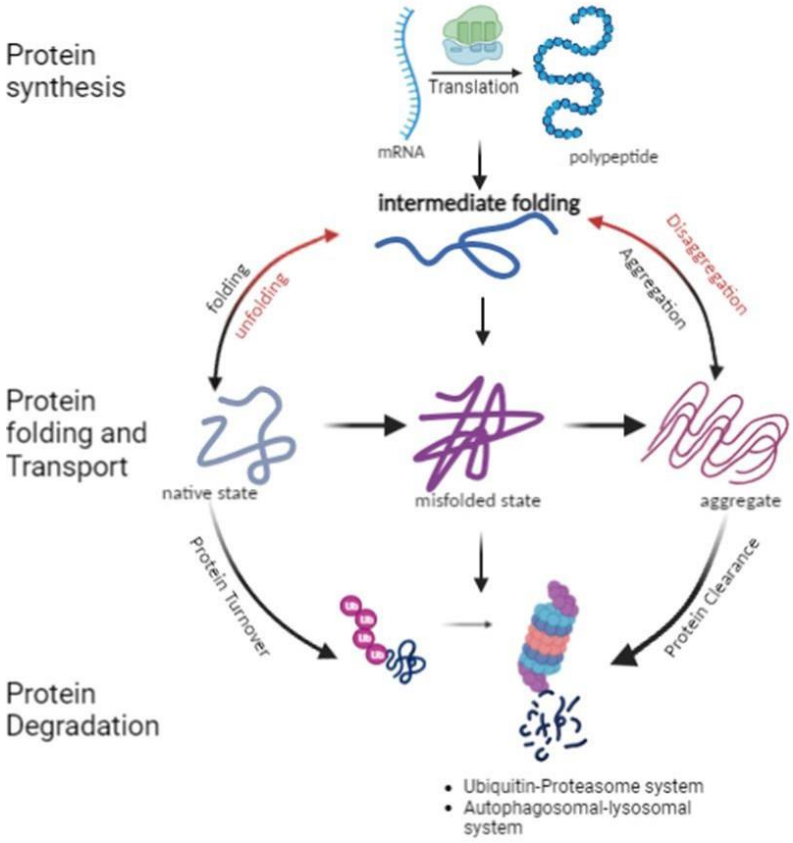

Figure 3 Shows a schematic representation of the proteostasis process in the cellular level.
Proteostasis network contains the different components such as Protein Synthesis, Protein folding/ transport and Protein degradation required to orchestrates the functions and process in the cells to navigate levels of protein in their native state. Illustration done using biorender.com.

1.5.1. Protein Synthesis

Protein synthesis is a crucial process of making proteins that are essential for the cells and the body to perform various biological functions. The process involves two significant steps: transcription and translation. Once the mRNA is transcribed, translation occurs in three stages: initiation, elongation, and termination. The process involves DNA being synthesized into mRNA in the nucleus, then transported to the cytoplasm to bind to ribosomes. Then, the second part of the process occurs, where the amino acids are activated and transfer to tRNA;

upon codon-anticodon match of the tRNA delivery, a polypeptide chain is formed. Finally, due to chain termination, proteins are translocated to the target site[16, 17].

The validation study of protein synthesis is fundamental yet complex investigation in eukaryotes to produce evidence. Traditionally, the protein synthesis rates have been studied using radiolabeled amino-acid tracers in experimental models. Although well-established and successful, the method proved to be expensive, time consuming and most importantly not excluding the potential risks of using the radioactive substances. In addition, the method was also reported to have limitations when measuring newly synthesized proteins at single-cell levels[15, 17]. Therefore in the recent decade, a non-radioactive method of measuring of newly synthesized proteins has emerged, which performed the detection and quantifying the global naïve proteins that are synthesized in homogenous and heterogenous cell populations known as SUnSET (surface sensing of translation) assay[18].

SUnSET assay is performed using puromycin, which is an amino nucleoside antibiotic produced from Streptomyces alboniger. Puromycin has a structural analogy with aminoacyl-tRNA that inhibits the protein synthesis by mirroring the 3' end of the amino acylated-tRNA that participates in delivery of the amino acid to elongating ribosomes during the translation elongation process (also shown in Figure 4). Since the peptide bond cannot be cleaved, this resulting in irreversible premature termination of translation. It is a significant tool that validates the changes in global translation [19].

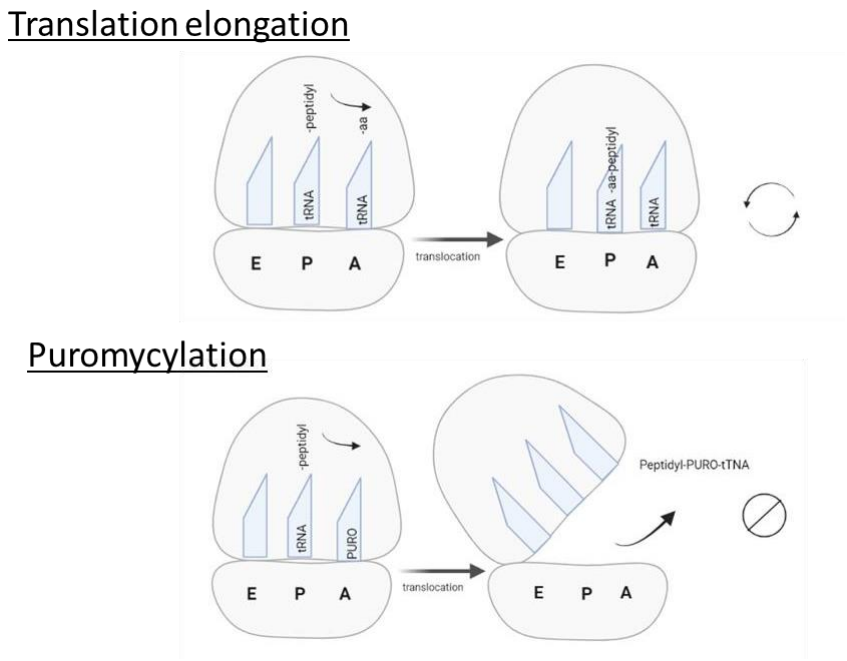

Figure 4: Puromycylation demonstrated was adapted from [19]
Puromycylation is process of mimicking the amino acylated t-RNA transfer in elongating ribosomes, therefore leading to premature termination of translation due to non-cleavage of the peptide bond formation. Illustration was created using Biorender.com

1.5.2. Protein Degradation

Most cellular processes have been shown to be dependent on the rate of protein synthesis or rate of protein degradation, affirming their role in maintaining homeostasis. Therefore, the cohesion of proteins contributes to a potential mechanism of gene expression, indicating the importance of protein degradation in the regulatory mechanism in vivo [20, 21]. There have been increasing studies suggesting that the dynamic changes contributing to the stability of the protein in vivo have led to selective proteolysis at different stages of the cell cycle.

Protein degradation can be described as the removal of unrequired or damaged cells, or faulty cells to maintain cellular homeostasis, which most of the intercellular processes are ATP-dependent. However, the role of intercellular proteins in complex mechanisms remains poorly understood, especially when studies apply the in vivo proteolytic cellular activity to in vitro studies[21, 22].

1.5.3. Autophagy

Autophagy is a Greek term, which translates to 'self-degrading.' This process involves the degradation and recycling of cellular components [23, 24]. Over a period of time, researchers have investigated the immense contributions of this process in molecular biosciences, providing some deep understanding of the mammalian cellular system. Autophagy has three main types: microautophagy, macroautophagy, and chaperon-mediated autophagy. All these types predominately perform the transport of cytosolic cargo to the lysosomes[25].

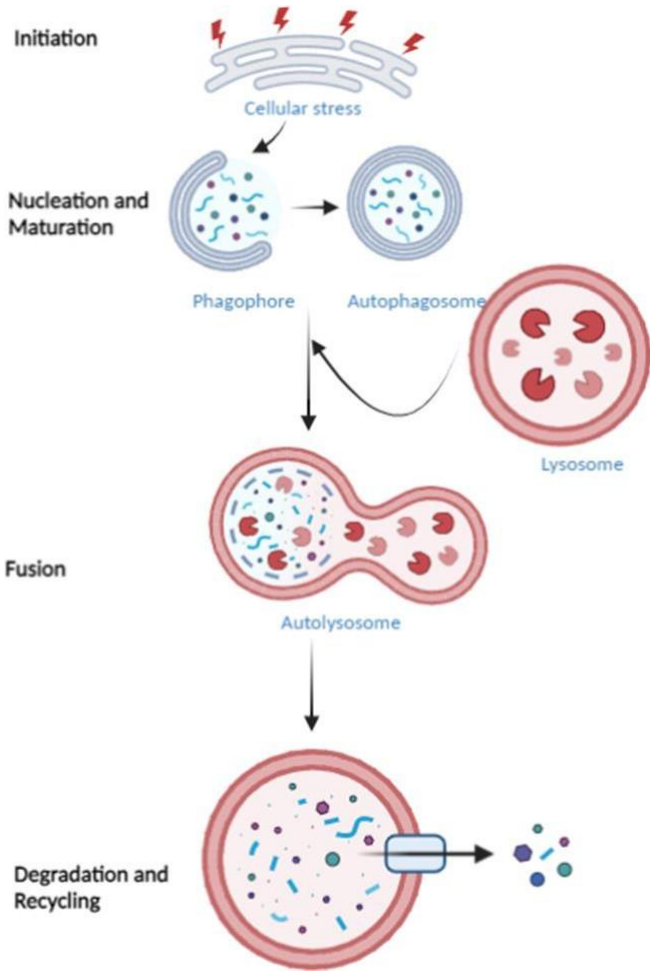

Figure 5 shows an illustration of the process of autophagy of cellular components.
Autophagy is multi-step process which includes sequential movements like nucleation of the a phagophore structure, maturation of the autophagosome, autophagosome fusion with lysosome and the degradation and recycling of the nutrients. Created using biorender.com

Autophagy is mediated by a double membrane organelle called autophagosomes, which engulfs the phagophore that contains the cargo from the intracellular structures like ribosomes and protein aggregates[25, 26]. Autophagy is described as a nonselective process in contrast to ubiquitination, in which only the ubiquitinated proteins are selected for proteasome degradation. Post maturation of the autophagosomes, the fusion of the double-membrane to lysosome is designated, (as illustrated in Figure 4) leading to the degradation of the autophagosome constituents by the lysosomal acid proteases[24, 26].

Subsequently, lysosomes then distribute the cellular by-products and the amino-acids to the cytoplasm, which is eventually re-used for further construction of macromolecules or/and metabolism. Therefore, autophagy is considered as a recycling process which filters the degraded and unwanted proteins. The induction of autophagy and depletion has also shown to promote ATP metabolism and cellular viabilities[24, 25].

Autophagy or auto-phagosome formation is detected using LC3b (microtubule-associated protein light chain 3) and p62/SQSTM1 (sequestosome1). LC3b is a cytosolic protein; when autophagy is induced, it is proteolytically cleaved by Atg4, a cysteine protease, to engender LC3b-I. LC3b-I, upon activation, is transported to Atg3, a carrier protein where phosphatidylethanolamine (PE) is conjugated to the carboxyl glycine, producing LC3b-II. The whole process and generation of LC3 are highly active during autophagy, making it a pivotal factor in measuring the autophagy levels in the target cells[23]. In addition, the p62 protein, which is a selective marker for autophagy and is utilized as a cargo receptor upon oxidative stress or other stressors, induces autophagic degradation of ubiquitinated targets[27].

1.5.4. Unfolded Protein Response

The endoplasmic reticulum (ER) plays a crucial role in maintaining protein homeostasis [28]. Proteins are translocated in an unfolded state through an essential secretory pathway into the ER from the cytosol, where they undergo chaperone-related folding to attain pertinent conformation. As a part of protein synthesis, protein misfolding has a higher tendency to have errors compared to transcription or translation [29]. The accumulation of these misfolded proteins in the ER lumen results in ER stress.

ER stress triggers the unfolded protein response (UPR), a cascade of various network transductions aimed at preserving proteostasis and maintaining ER functions. This process is important for ensuring proper proteostasis, however, in cases where ER stress persistent and reaches elevated levels, it can lead to various diseases such as metabolic disorders, cancer, and neurodegenerative diseases [28, 29].

Evidence suggests the involvement of the UPR process in fibrosis of many organs such as the liver, heart, lungs and kidney [28]. ER is a very well-coordinated system that involves in maintaining the functions of protein synthesis, metabolic supply of the cell, calcium- ion exchange; and disruption to any of these functions activates the UPR[30].

The UPR has three majors signaling pathways induced by ER transmembrane proteins: (a) PKR-like endoplasmic reticulum kinase (PERK), (b) activating transcription factor 6 (ATF6), and (c) inositol requiring enzyme 1 α (IRE1α) [28-30]. Binding immunoglobulin protein (BiP) is an HSP70 protein functions as ER sensing chaperone, which is bound to all of the ER transmembrane proteins during the non-stressed state of a cells, helping the maintenance of the protein homeostasis. Once the UPR is activated due to induced ER stress, BiP tends to segregate from the sensors, and thereby activating the downstream adaptive UPR signaling cascades [28, 31].

One of the protein kinases that is activated upon ER stress is PERK, which goes through auto-phosphorylation[32]. Following dimerization, activated PERK phosphorylates the α-subunit of eukaryotic translation initiation factor 2α (eIF2α) at serine 51 (Ser51), leading to the attenuation of the translation (Figure 6). Although phosphorylation of eIF2a inhibits global protein synthesis, it potentially up-regulates the activating transcription factor 4 (ATF4), a transcription factor crucial for expression of genes associated with maintenance of protein

quality control or homeostasis [28, 32, 33]. Additionally, ATF4 has downstream regulation of C/EBP homologous protein (CHOP), a pro-apoptotic factor that mediates cell death upon ER stress activation. CHOP has been shown to contribute to expression of genes that encode proteins for proliferation, energy metabolism, and differentiation. There have been studies by researchers claiming to show that CHOP-knockdown mice tend to show resistance to ER-induced apoptosis[34, 35].

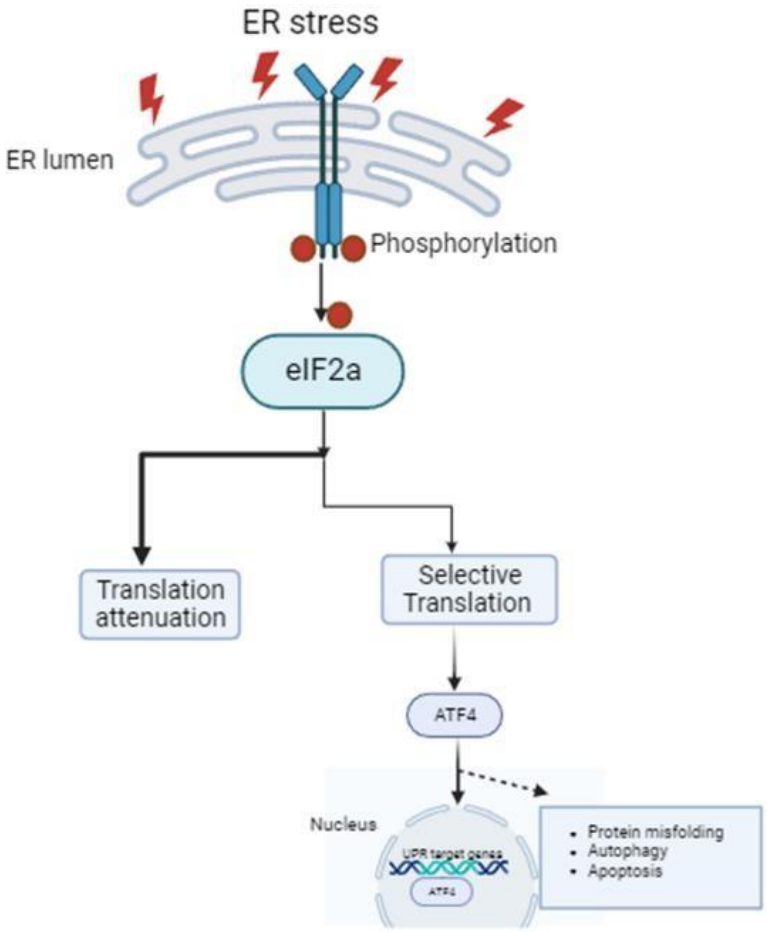

Figure 6: Schematic flow of the PERK pathway during ER stress.
ER stress and the UPR are regulated by three ER transmembrane proteins: inositol requiring enzyme 1(IRE1), protein kinase R-like ER kinase (PERK), and activating transcription factor 6 (ATF6). PERK endures auto-phosphorylation which then stimulate the eIF2a phosphorylation consequentially leading to translation attenuation or upon selective translation initiating activation of ATF4. Illustration done using Biorender.

1.6. Eukaryotic Elongation Factor 1 alpha

The synthesis of proteins is a highly conserved process carried out through three stages: initiation, elongation and termination. The majority of the translation occurs in the cytosol or the ER bound at ribosomes[36]. There are some pivotal cellular components which are translated within the mitochondria, where they also anchor their own translation machinery including different ribosomal subunits, initiation factor and tRNAs[37].

Translation elongation requires several soluble proteins called eukaryotic elongation factors. Eukaryotic elongation factor 1 alpha (eEF1A) is known to be a GTP-binding protein and a homolog of the bacterial protein EF-TU[38]. eEF1A has two distinctive isoforms: eEF1A1 and eEF1A2. Both these isoforms exhibit very subtle structural differences in the protein surfaces with variant amino acid residues not drastically affecting post-translational modifications[38, 39]. However, they have distinctive expressions; eEF1A1 is ubiquitously expressed in all cell types except in adult skeletal muscle, cardiomyocytes, and neurons. In contrast, eEF1A2 is only expressed in cardiomyocytes, skeletal muscle cells and neurons[38, 39].

Pseudogenes are considered junk DNA of parental protein-coding genes, which cannot encode a protein or have no potential biological competence [40]. However, in recent studies, evidence shows that both pseudogene-derived transcripts and pseudogene-derived proteins can display an essential biological role in the cell[40-42]. There have also been demonstrations of the pseudogenes' role in both negative and positive biological roles in the cells[40].

The role of pseudogenes at the RNA level affects the expression of its parental gene and different mechanisms, including one or more of its transcripts[43]. On the protein level, pseudogenes-derived proteins could positively or negatively affect the activity of the parental protein[40, 43]. Additionally, pseudogene-derived proteins tend to have biological activity in

tissues where the parental gene is not expressed. The same protein product may gain activity only upon stimulated pathological conditions such as in cancer[40, 43].

The EEFs have been reported to carry many pseudogenes; eef1a1 isoform specifically has a high number of pseudogenes[40, 44]. The associated pseudogenes are categorized as retro pseudogenes, classified into processed pseudogenes, unprocessed pseudogenes, and transcribed unprocessed pseudogenes [40, 45]. Retro pseudogenes can be described as genes that are localized in a different location compared to their parent gene and which are reported to be actively transcribed, or have one or more transcripts, or could be a result of gene duplication and found on the same chromosomes of their parental genes[40, 46, 47]. Therefore, among all EEFs, eEF1A1 has been reported to have an abundant number of pseudogenes. These pseudogenes in the human genome are not necessarily due to evolution but may also have other factors contributing, such as high transcription of its parental gene[48].

eEF1A requires guanine nucleoside exchange factor (GEF-eEF1β$\alpha\gamma$) to promote GDP release and reactivate the protein for aminoacyl-tRNA delivery. The function of eEF1A can be classified into two major functions, canonical and non-canonical.

1.6.1. Canonical Functions of eEF1A

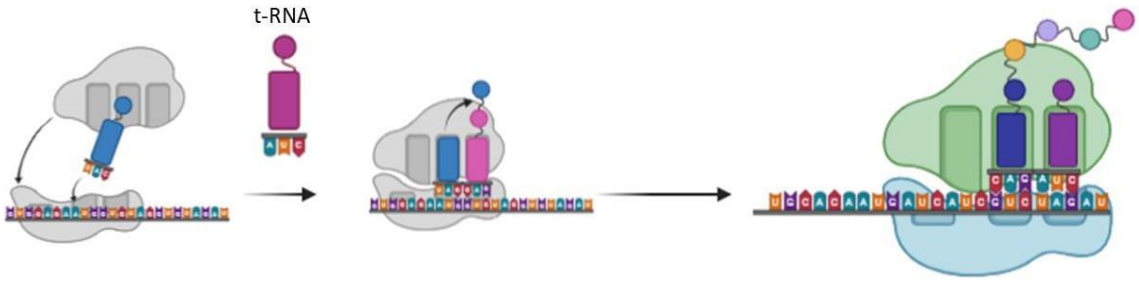

Figure 7: Canonical function of eEF1A
eEF1A transports the aminoacyl-tRNA to the A-site of the ribosomes. Upon identifying the codon and anti-codon match leading to the formation of peptide bond contributing to the elongation process. Illustration created using Biorender.com

eEF1A is primarily known for its canonical function, which involves delivering the aminoacyl-tRNA to the ribosomes. During elongation, eEF1A transports the cognate aminoacyl-tRNA to the A-site of the ribosomes[39]. Once the codon and anti-codon match is established, eEF1A releases itself from the ribosomes after transportation of the aminoacyl-tRNA. This leads the formation of a peptide bond contributing to the elongation of the evolving polypeptide chain (Figure 7). As the elongation process of translation continues, elongation factor 2 (EF2) acts and it catalyzes the movement of the polypeptide-tRNA-mRNA complex from the A-site to the P-site of the ribosomes, allowing the next codon to position itself in the A-site and for the process to repeat[39].

1.6.2. Non-canonical functions of eEF1A

In recent decades, the non-canonical functions of eEF1A have been extensively investigated apart from the known canonical role of eEF1A (Figure 8-A).The transport of cellular cargoes into and out of the nucleus has known to be an essential part of the biologic process[49]. In mammalian cells, eEF1A1 have reported to mediate nuclear export of proteins[49, 50]. Studies

have indicated a key role of eEF1A1 interacting with other proteins in the cytoplasmic side and also in the nuclear membrane making the function essential in transcription-dependent export pathway machinery (Figure 8-B)[39, 49, 51].

The abundance of eEF1A in close proximity to ribosomes might facilitate a potential role in protein degradation. Autophagy can also induce apoptosis, cellular events that culminate in the elimination of dead cells or unrequired cells [32]. Dapas et al. showed how targeting eEF1A promoted autophagy associated with protein quality control, leading to the downregulation of autophagy markers (LC3bII) upon protein knockdown. The role of each isoform may differ in the process of differentiation, proliferation, and apoptosis (Figure 8- C and D) as they still need to be well defined [39, 52].

Yang et al. isolated eEF1A and associated it with an actin-binding protein from the slime mold, Dictyostelium discoideum [53]. eEF1A is shown to both bundle and bind to actin, but not in the presence of aa-tRNA, implying the function of the actin-binding is independent of the deposition of the aa-tRNA undergoing GTP activity (Figure 8-E). Studies have indicated the direct and indirect interaction of eEF1A with actin-binding mediated via the Rho/Rho kinase pathway[54].

As demonstrated by its abundant accumulation in f-actin bundling, leading to the formation of stress fibers, eEF1A gives rise to potential viral transcription and morphogenesis[39, 54, 55]. eEF1A has shown to play a significant role in human respiratory syncytial virus (RSV) replication, and also contributed in detection of the localization of the eEF1A in f-actin stress fibers (Figure 8-F). This indicated that eEF1A is crucial not only for maintaining the formation of stress fibers but also RSV assembly and the release[54].

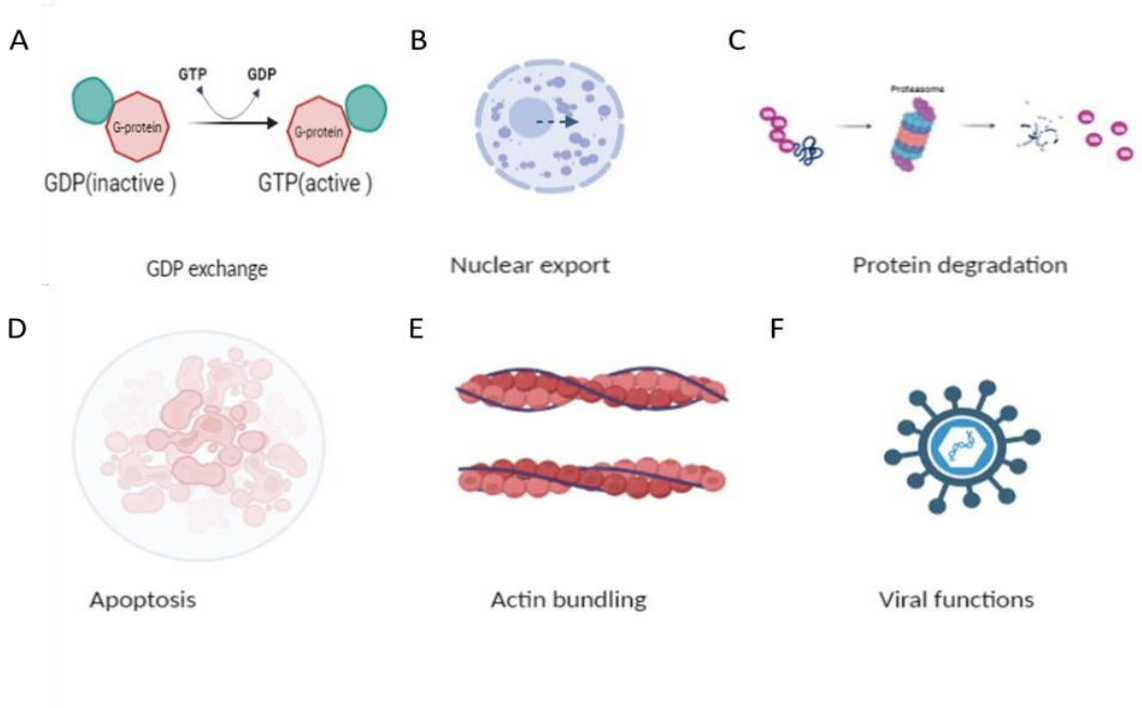

Figure 8: A-F are some of the investigated Non-Canonical functions of eEF1A

eEF1A non- canonical functions described individually A-GDP exchange promoted by the GEF eEF1B, B-another non-canonical function involves role eEF1A plays in Nuclear export process, C-involvement in protein degradation process, D-apoptosis, E-Actin bundling and binding and also other cytoskeletal components and F- playing a crucial role in viral infections life cycle. Illustration created using Biorender.com

2. Aims of the Study

Several studies suggest that eEF1A plays a crucial role in non-canonical functions independent of its most well-known canonical function in translation elongation. In order to evaluate the function of eEF1A in cardiac fibrosis, it is fundamental to understand its role in cardiac fibroblast. To this end, in vitro models were employed with the following aims:

- To investigate the role of eEF1A in fibroblast activation and myofibroblast differentiation.
- To identify the underlying mechanisms involved in the contribution of eEF1A in fibrosis.

By addressing these questions, a better understanding of whether eEF1A is a viable target to treat cardiac fibrosis can be gained. Additionally, further investigation could involve in vivo experiments using a mouse model of cardiac fibrosis.

3. Materials

3.1. Reagents

Table 1:List of reagents

Compound	Company	Catalogue number
Agarose-500g	Bioline	BIO - 41025
Ponceau S	Sigma Aldrich	P7170-1L
Bovine Serum Albumin (BSA)	PAN	P06-1391100
Triton-100x	Carl-Roth	30512
PBS	Linaris	GBP1626LK
Sodium Pyruvate	Thermofischer	S8636-100ML
L-Glutamine	Thermofisher	25030024
Beta-Mercapthol	sigma	M3148-100ml
Pencillin Strep	Thermofischer	15140-122
Non-essential amino acid	Thermofischer	11140-035
Methanol	Carl-Roth	8388.5
Ethanol 70 %	Carl-Roth	T913.3
Ethanol 100%	Carl-Roth	K928.4
DMEM-high glucose	PAN-Biotech	P04-03500
Fetal Calf Serum	Thermofischer	10270-106
Midori green	Biozym	617004
Gene Ruler 100bp DNA Ladder	Thermo Scientific	SM0242
GeneRuler 1 kb DNA Ladder	Thermo Scientific	SM0313
Ambion-nuclease free water	Thermo scientific	R0582
Injection water	Serumwerk Bernburg AG	626544
Power-up Sybr green	Thermo scientific	15360929
Paraformaldehyde	Carl Roth	0335.3
Recombinant mouse TGFb2 protein	R&D systems	7346-B2-005
BCA protein Assay Kit	Thermo Fisher	23227
cDNA Synthesis Kit	Thermos Scientific	K1652
Percoll 1l	GE Healthcare/ Sigma	17-0891-01
GE Amersham Ecl Prime Western Blotting Detection Reagent	Sigma-Aldrich Chemie GmbH	GERPN2236
Lipofectamine™ 3000 Transfection Reagent	Invitrogen	L3000015
Liberase TH	Roche	5401151001
Collagenase Typ 2	Worthington	LS004176

Vectashield HardSet Mounting Medium with DAPI	Vector Lab	VEC-H-1500
ProSieve QuadColor Protein Marker, 4.6 - 300 kDa	830537 (00193837)	Biozym
Apo-ONE® Homogeneous Caspase-3/7 Assay	G7790	Promega
AdEasy viral titer assay	972500	Agilent

3.2. Antibody list

Table 2: Primary antibody list for Immunofluorescence

Antibody	Company; Catalogue Number	Dilution
Collagen 1 a1	Santa cruz; sc-293182	1:50
eEF1A	Santa Cruz; sc-21758	1:50
Alexa Fluor® 488 Phalloidin	Life technologies; A12379	1:40
Alexa Fluor® 555 Phalloidin	Life technologies; A34055	1:40
Ribosomal Protein S6	Cell Signaling; 2217	1:100
α-Smooth muscle actin	Abcam; ab7817	1:100

Table 3: Secondary antibody list for immunofluorescence

Antibody	Company; Catalogue Number	Dilution
Alexa Fluor anti-mouse 488	Cell Signaling; 4408	1:200
Alexa Flour anti-rabbit 555	Cell Signaling; 4413	1:200
Alexa Flour anti-mouse 555	Cell Signaling; 4409	1:200
Alexa Flour anti-Rabbit 488	Cell Signaling; 4412	1:200

Table 4 : Primary antibody list for Western blot

Antibody	Company; Catalogue Number	Dilution
Beta-Actin	abcam; ab115777	1:1000
Beta-Tubulin	Cell signaling; 2146	1:1000
Collagen 1 a1	Santa cruz; sc-293182	1:1000
eEF1A1	Proteintech; 11402-1-AP	1:2000
eEF1A2	Proteintech; 16091-1-AP	1:2000
eEF1A1	Santa Cruz; sc-21758	1:5000
eEF2	Cell signaling; 2332	1:1000
GAPDH	Fritzgerald; 10R-G109a	1:3000
KDEL	Enzo Life Sciencies; ADI-SPA-827-D	1:1000
LC3b	Cell Signaling; 3868	1:1000
SQSTM1/p62	Sigma; P0067	1:1000
PCNA	Santa cruz; sc-56	1:1000
Puromycin-12D10	Millipore; MABE341	1:5000
Ribosomal Protein S6-total	Cell Signaling;56S10	1:2000
Ribosomal Protein S6-Phospho	Cell Signaling; 2317S	1:2000
α-Smooth muscle actin	Abcam; ab7817	1:1000

Table 5: Secondary antibody list for Western blot

Antibody	Company; Catalogue Number	Dilution
Anti-mouse IgG (HRP-linked)	Cell signaling;7076S	1:5000
Anti-mouse IgG2a (HRP-linked)	Cell signaling; 33416	1:2000
Anti-rabbit igG peroxidase	Thermo Scientific; NA934V	1:5000

3.3. SiRNA

Table 6: List of siRNAs

Gene	Company; Host	Catalogue number
eEF1A1	Horizon; rat	L-091712-02-0010
eEF1A2	Horizon; rat	L-089975-02-0010
Control	Horizon; rat	D-001810-10-20

3.4. Primers

***Table 7*: Primer list**

Name	Forward Sequence	Reverse Sequence	Species	Company
eEF1A1	ACGAGGCAATGTTGCTGGTGAC	GTGTGACAATCCAGAACAGGAGC	mouse	Sigma
eEF1A2	ATGCTCCAGGACACCGAGACTT	GTTTGCCCGTTCTTGGAGATGC	mouse	Sigma
Collagen 1a1	CCGCTGGTCAAGATGGTC	CCTCGCTCTCCAGCCTTT	mouse	Sigma
Collagen 3a1	AAGGCTGAAGGAAACAGCAA	TGGGGTTTCAGAGAGTTTGG	mouse	Sigma
Acta2	GTTGGTGATGATGCCGTGTT	CTTCGCTGGTGATGATGCTC	mouse	Sigma
SM22	GCCACACTGCACTACAATCC	CCAGTCCACAAACGACCAAG	mouse	Sigma
FN1	TGTGACAACTGCCGTAGACC	TGGGGTGTGGATTGACCTTG	mouse	Sigma
Tgfb1	TGATACGCCTGAGTGGCTGTCT	CACAAGAGCAGTGAGCGCTGAA	mouse	Sigma
Tgfb2	CAGCGCTACATCGATAGCAA	CCTCGAGCTCTTGCTTTTA	mouse	Sigma
Tgfb3	GCCTCTCAAGAAGCAAAAGG	GATCCTGCCGGAAGTCAATA	mouse	Sigma
Chop	CATGAACAGTGGGCATCACC	GCTGGGTACACTTCCGGAGAG	mouse	Sigma
Grina	CAAGCCCCTATGCCTCCCTAT	GGCCCTTGAGGGTAACCAC	mouse	Sigma
Puma	ACGACCTCAACGCGCAGTACG	GAGGAGTCCCATGAAGAGATTG	mouse	Sigma
Gapdh	CCGCATCTTCTTGTGCAGT	CATCACCTGGCCTACAGGAT	mouse	Sigma
Hprt	AAGCTTGCTGGTGAAAAGGA	TTGCGCTCATCTTAGGCTTT	mouse	Sigma
eEF1A1	CGGCCACCTGATCTACAAAT	CACGCTCAGCTTTCAGTTTG	rat	Sigma
eEF1A2	CAAGTTTGCCGAGCTAAAGG	CGCTCTTCTTCTCCACGTTC	rat	Sigma
Collagen 1a1	CAGGTGTGGCTGAAGAATGG	GCACTTCGGTTTCTGGGATC	rat	Sigma

Collagen 3a1	GGAAACCGGAGAAACATGCA	GCCAGCTGTACATCAAGGAC	rat	Sigma
Acta2	GCATCCACGAAACCACCTAT	GCGTTCTGGAGGAGCAATAA	rat	Sigma
FN1	TGCTTCCCGTTGTCAAAACA	ACTCAAGATGCTCAGGGGTC	rat	Sigma
Tgfb1	ACCAACTACTGCTTCAGCTCCACA	TGTACTGTGTGTCCAGGCTCCAAA	rat	Sigma
Tgfb2	TAACATCTCCAACCCAGCGCTACA	ATCCCAGGTTCCTGTCTTTGTGGT	rat	Sigma
Tgfb3	CTTACCTCCGCAGCTCAGAC	GTCAGAGGCTCCAGGTCTTG	rat	Sigma
Chop	ACAAGCTGAGCGACGAGTAC	CATCAACAGCAACAACCCCG	rat	Sigma
Gapdh	ACCACCATGGAGAAGGCTGG	CTCAGTGTAGCCCAGGATGC	rat	Sigma
Hprt	GCAGACTTTGCTTTCCTTGG	CCGCTGTCTTTTAGGCTTTG	rat	Sigma

3.5. Consumables

Table 8: Consumables list

Name	Catalogue Number	Company
Cell culture dish-60mm	628161	Greiner
Cell Culture dish 100mm	833.902	Sarstedt
6 well plate	833.920.005	Sarstedt
PCA slides	94.6140.402	Sarstedt
Cell scrapper	83.395	Sarstedt
Pasteur pipette-2ml	861.252.011	Sarstedt
Serelogical pipettes-2ml without filter	86.1252.011	Sarstedt
Serelogical pipette 5ml	861.253.001	Sarstedt
Serelogical pipette 10ml	861.254.001	Sarstedt
Serelogical pipette 25ml	86.1685.001	Sarstedt
Serelogical pipette 50ml	861.256.001	Sarstedt
Cover slips	BB024050A1	Menzel
T75-flask	833.911.002	Sarstedt
Cryotubes	72.379.992	Sarstedt
Eppendorf tubes (1.5ml)	0030123328	Eppendorf
Eppendorf tubes (2ml)	30120094	Eppendorf

Eppendorf tubes (5ml)	30119401	Eppendorf
Pipette tips (10µl)	70.3010.255	Sarstedt
Pipette tips (30µl)	F171303	Gilson
Pipette tips (100µl)	703.030.355	Sarstedt
Pipette tips (200µl)	703.031.255	Sarstedt
Pipette tips (1000µl)	703.060.255	Sarstedt
Falcon tubes 15ml	62.554.009	Sarstedt
Falcon tubes 50ml	62.547.254	Sarstedt
PVDF membranes	IPVH00010	Carl-Roth
Parafilm	PM-996	Carl-Roth
Whatman filter paper	11350394	Cytiva
Syringe-5ml, 10ml,20ml	NJ-4606051	B.Braun Deutsch
Syringe needles	C724.1	B.Braun
Magnetic stirer	1PK8.1	IKA
Filter 0.2µm	7.616 308	Buddeberg
qPCR plate	721980	Sarstedt

3.6. Laboratory Equipment

Table 9: Laboratory equipment's list

Name	Company
Incubator	Binder
Cell culture-37°C 5% CO_2	Binder
qPCR	Agilent.AriaMx
Mini-PROTEAN 3 Multi-Casting Chamber	BioRad
Pipette-set	Gilson
Mini-PROTEAN® Spacer Plates with 1.0 mm Integrated Spacers	Biorad
Mini-PROTEAN® Comb, 15-well, 1.0 mm, 26 µl	Biorad
Laminar flow bench	Thermo
Water bath	Thermo fisher
Weighing scale	sartoriuos
Electrophoresis chamber and system	Biorad
Plate reader	Teccan spark
membrane Imager	Am

Centrifuge	Thermoscientefic
Fluorescence widefield Microscope	DMi8- Leica systems
Confocal TC SP8 microscope	Leica systems
Millipore water	MilliQ
-20°C freezer	Liebherr
-80°C Freezer	ThermoScientific
Liquid Nitrogen Tank	ThermoScientific
2°C- 8°C Fridge	Liebherr

4. Methods

4.1. Approval for use of mice/rats for experiments

The animals (mice and neonatal rats) were used with approval from animal welfare commission, Karlsruhe, Germany. The neonatal rats were obtained from Janvier WT. For the isolation of cardiac fibroblast and mouse embryonic fibroblast cells were isolated from neo-p-Flox transgene mice in an approved animal proposal from the Regional Council Karlsruhe and the Lower Saxony Office for Consumers Protection and food Safety, Germany approved protocols I-22/03.

4.2. Genotyping for Mice

Genotyping of the mice was done using the standard pcr protocol:

Table 10: Genotyping for eEF1A flox/flox mice reaction mix

Reagents	Volume (µl/sample)
5x- green buffer	4
Magnium Chloride 25mM	2
dNTPs 10nM	0.40
Primers-forward 10µM	0.40
Primers-Reverse 10µM	0.40
DNA	1
water	11.68
Go-Taq polymerase	0.12

Table 11: Genotyping primers for flox/flox

Name	Forward Sequence	Reverse Sequence	species
eEF1A1	GTAGGGTGGTAGGAATACCTTCAATA	AAACTTAGGCCACCTGTTTTCATCT	mouse
eEF1A2	GAAATATAGGTCACATGGGCCAA	GCTCACACAGACGGTCTGGCTTC	mouse

Table 12: Thermal cycler program for genotyping flox/flox eEF1A

Temperature	Time	Cycle
94°C	5min	
94°C	30sec	x33
62°C	35sec	
72°C	35sec	
72°C	5min	
hold 4°C		

4.3. Cell culture and Cell isolations

4.3.1 Neonatal Rat cardiac Fibroblast cell isolation

Neonatal rat cardiac fibroblast (NRcFB) from one to three-day-old rats were used for the isolation. The rats were decapitated with scissors, and the heart was taken into cold 1x ADS. The atria were removed before mincing the heart into small pieces. The pieces were then collected into the enzyme solution (Collagenase Type II and Pancreatin). The Fibroblast isolation was done by the percoll gradient method. Fibroblasts were subjected to pre-plating in the plating medium (DMEM+M199+10%FCS) for 2 hours after isolation. The pre-plating is done in order to remove contamination of other cell types. After two hours medium is changed with DMEM + 10%FCS.

4.3.2 Mouse Embryonic Fibroblast

Mouse embryonic fibroblasts (MEF) were isolated from eEF1A1/A2- flox/flox mice (BL6), and WT (BL6) mice. After pairing with male mice female mice were sacrificed after 12.5 days to isolate MEF from respective embryos. The embryos were isolated, and the head and organs were removed from the carcass and carcass was then dissociated using Trypsin in the cell

culture plate individually, incubated at 37℃ for 10 mins, and then the reaction was stopped by adding the Medium containing 10% FCS. Then cells from the carcass were allowed to grow for 2 to 5 days with changing medium every two days. The MEF was stable to freeze and to passage until P5.

4.3.3. Adult Mouse Fibroblast

Mice (BL6) from eEF1A1/A2- flox/flox of 8 weeks to 12 weeks old were used for isolating the cardiac fibroblasts. The hearts taken from the mice are put into a dish with cold 1xPBS. Hearts were cut into small pieces with scissors and transferred into a falcon under sterile conditions. The tissue pieces are treated with enzyme solution (SADO mix and Liberase-DH). The cells are collected with five consecutive digestion steps before adding horse serum to stop the reaction. The cells are all collected in a falcon and placed in an ice box. Finally, the cells are plated into a cell culture dish—3 hearts in one 10cm dish with DMEM in 10%FCS. The cells are cultured for five days until the fibroblast attains confluency, with changing fresh medium every two days. This model is used as a tool for predictive translation studies.

4.4. Adenovirus production of Cre-recombinase and beta-Galactosidase

For the knocking down of eEF1A, adenovirus-Cre recombinase was created and used in comparison to beta-Galactosidase as the control for related experiments.

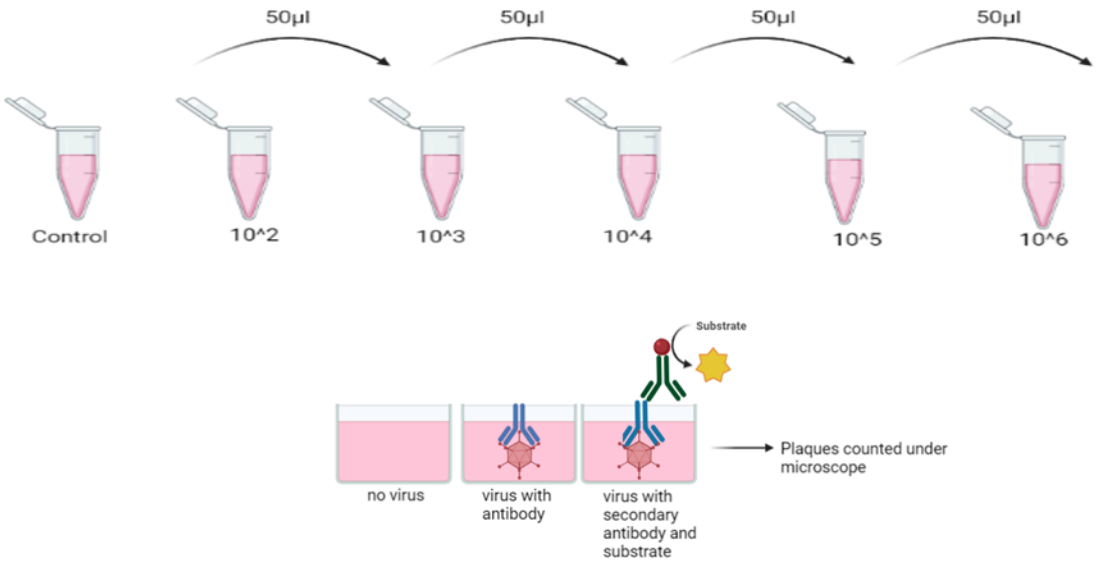

Figure 9: Scheme of flow for the Ad.Viral titration assay for Ad.βgal and Ad.Cre
Illustration created using Biorender.com

Titration of the virus was done using AdEasy viral titer assay. The adenovirus for Cre-recombinase was titrated using HEK-AD cells following the manufacturers' protocol for Agilent AdEasy Viral titration kit. The images were taken following the plaque staining protocol provided by the company in brightfield microscope leica DMi8. PFU (plaque forming units) was calculated by counting the plaques from Dilution 10^2 and 10^3 (shown in Figure 10) for Ad. Cre and Ad. β-Galactosidase (βgal) respectively.

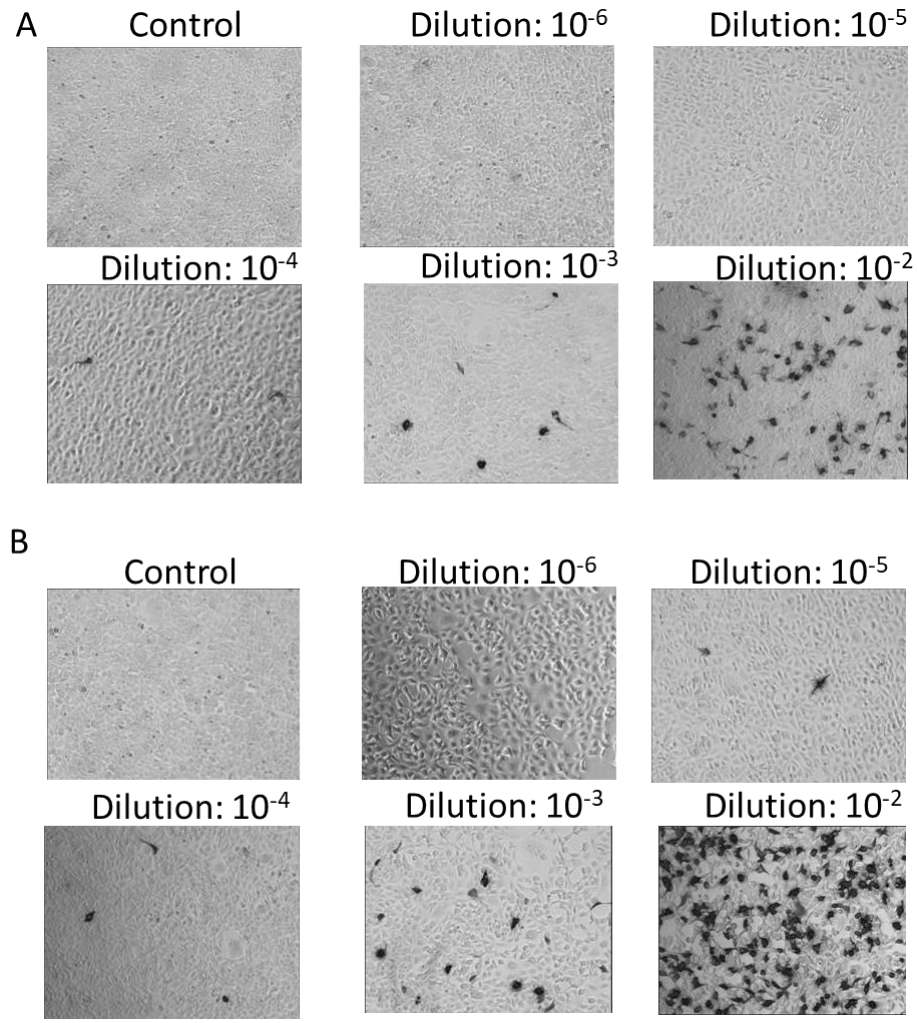

Figure 10: The plaques developed with viral titration assay.
Ad.βgal (A) and Ad.Cre (B)shown are brightfield images taken post the viral titration assay on HEK-293 cells respectively. Determination of MOI for each condition Ad. βgal and Ad. Cre was done based on the images shown here.

The PFU value was determined with this titration, and 50MOI was used in the calculation. The formula used for calculating PFU:

Number of cells * desired MOI =total PFU

(total PFU needed) / (PFU/ml) = total ml

50MOI has shown efficient Knockdown of approximately 50% at the protein level for the experiments.

4.5. Total RNA isolation for qPCR

RNA was isolated using the Macherey Nagel RNA nucleospin kit. Following the determination of RNA concentration, cDNA synthesis was generated for every sample for 100ng/µl.

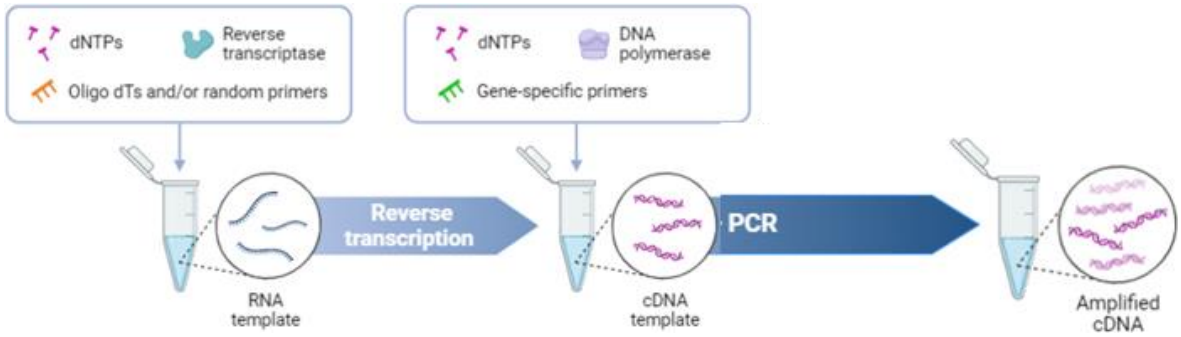

Figure 11: RNA isolation with two- step shown in this scheme.
The illustration is done with help of Biorender.com

Table 13: Master mix for cDNA synthesis

Reagents	Volume (in µl per reaction)
ddNTPs	1
Oligos	0.25
Random Primer	0.25
Water	3
Reverse Transcriptase-buffer	4
Reverse Transcriptase enzyme	1
Sample	10ng/well

4.6. Total Protein isolation for Western blot

4.6.1. Protein concentration measurement

Cells were lysed in RIPA buffer containing: 50mM Tris HCL(m/v) (pH 6.7), 2% SDS (m/v), and 20mM Glycerol (v/v) dissolved in water. Samples are then heated at 95℃ for 5mins and centrifuged 10mins at 13000rpm. Supernatant was then transferred into a fresh Eppendorf tube, and 6µl of each of the samples were taken to determine the concentration using BCA assay, and 5µg to 20µg of protein was loaded into the gels.

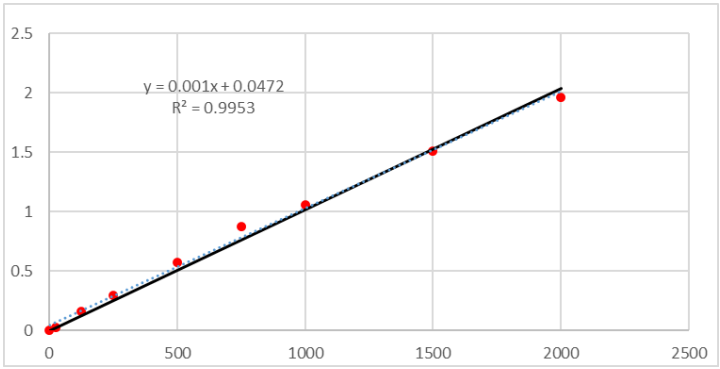

Figure 12: Shows the standard curve used to detremine the Protein Concentration for respective proteins.

Gel preparation as resolving gel was formulated according to the molecular weight of the different proteins. For LC3b, 13% gel was used; and for other proteins, 10% gel was used. For the SUnSET assay, 7.5% to 8% gel was used; the only difference in this experimental setup is that puromycin was added 30 minutes before harvesting the cells. The cells were lysed, and protein was extracted. Stacking gel was constant for all the proteins with 5% in a 10mm glass chamber. The transfer was done in a wet chamber at 100V for 1 hour and 15min using a PVDF membrane. Blocking was done in 3%BSA-TBST for 1 hour, and respective primary antibodies were added for overnight incubation at 4℃. Secondary antibodies corresponding to the primary antibodies were incubated at room temperature for 1 hour. After washing the

membrane three times with 1x-TBST, a blot was developed using ECL in Amersham Imager 600 (GE Healthcare Life Sciences).

4.6.2. Western Blotting Analysis

All the developed blots in Image J. Puromycin blotting for SUnSET was analyzed by measuring each complete lane as individual input and normalized with GAPDH of the respective sample. All the proteins were analyzed and quantified in GraphPad prism 8.0.

4.7. Immunofluorescence staining

Immunofluorescence staining was performed on all cell types in PCA 4 well-chamber slides after fixing in 4%PFA for 15mins at room temperature. For permeabilization, 0.3%Triton-X100 in PBS was applied for 5 mins, room temperature. After permeabilization, the cells were washed for 5 mins with PBS, repeated this step 3 times. Blocking of the samples was done in 3% BSA in PBS for 30mins at room temperature. Antibody was applied with respective dilution; eEF1A1 (1:50), Phalloidin 555 (1:40), Ribosomal protein S6 (1:100), and Collagen 1a1 (1:50).

All the primary antibodies were incubated overnight 4°C and following with secondary antibody with individual host species for 2hr in room temperature.

All the slides were mounted with Vectashield mounting medium with DAPI covered with cover glass (thickness 1.5). The images were taken in Leica DMi8 and Leica SP8 (LIMA core facility, UMM) for immunofluorescence. For image analysis, pictures were analyzed in Image J and quantified.

4.8. Polysome Profiling

Polysome profiling was performed to analyze the ribosome run-off in primary cells- mouse embryonic fibroblasts. The appropriate time point to determine the cells post-knockdown was 48 hours. The cells were plated in 6cm dishes, first treated with harringtonine drug for 4 mins, 2 mins, and as control, no treatment dish was labeled as 0 min. Then all the dishes were treated with cycloheximide for 5mins, and washed the cells were with cold 1xPBS+chylohexamide. Cells were then harvested in a Polysome lysis buffer. Lysed cells are then centrifuged at 1000rpm for 10min. The supernatant was then transferred to the gradient (17.5% to 55% sucrose gradient) in a cold room. The gradients were centrifuged at 40000rpm at 4°C in an SW60 rotor (Acceleration:7, Deceleration:1) for 2.5 hours. Dr. Sonja Reiter recorded and prepared the gradients for the polysome profile.

4.9. Total protein Isolation for Proteomics

Adult mouse cardiac fibroblast samples, neonatal rat cardiac fibroblast samples, and mouse embryonic fibroblast were sent for proteomics analysis. The sample analysis and processing were done by the EMBL proteomic core facility. All the samples were lysed in the RIPA buffer, and protein concentration was determined, as mentioned in 4.4.1. For analysis, 20µg/50µl was provided to the core facility.

4.10. Cellular Function assays

4.10.1. Migration assay

Fibroblasts migrate upon activation. Scratch assays were performed to analyze the migratory effects in knockdown conditions with all the models (adult mouse, neonatal rat, mouse

embryos). The cells were seeded in the 24 well plates and treated with adenovirus-Cre/beta-Galactosidase in the case of adult mouse and mouse embryos; siRNA-eEF1A1, eEF1A2, and control were treated with neonatal rat fibroblasts. After 24h incubation, a sterile 200µm tip straight line was drawn in the middle of each well, and the corresponding medium was changed. Images were taken at 0 hours, 6 hours, 12 hour/18 hours, 24 hours and 30 hours. Mitomycin C (Sigma 2mg, M4287) was used to inhibit cells from proliferation. Closure of the scratch in control cells was determined at the end of the experiment, and the areas were analyzed and quantified in ImageJ and GraphPad Prism, respectively.

4.10.2. BrdU- Proliferation assay

Cell Proliferation was assessed using Cell proliferation BrdU ELISA-based assay (Roche, 11647229001). The basic principle of this assay is to track the nuclear DNA labeled with the thymidine analog with HRP-conjugated antibodies (working illustration shown in Figure 13). The assay was performed per the manufacturer's protocol, and the Spark Deccan plate reader determined colorimetry at 0 mins, 2 mins, and 4 mins, and the difference is calculated and quantified in GraphPad prism.

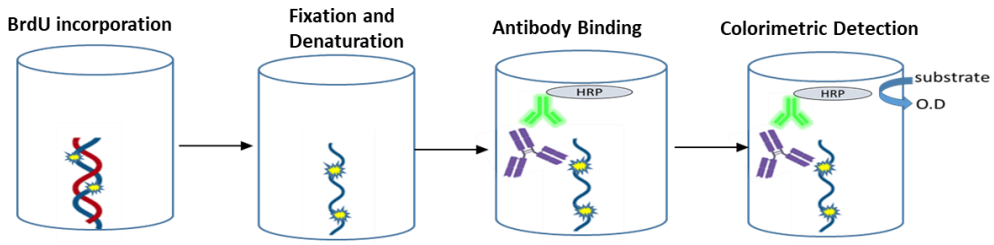

Figure 13: showing the working principle of the BrdU assay.
The nuclear DNA labeled with the thymidine analog with HRP-conjugated antibodies. The antibodies detection was determined by colorimetric plate reader at 570nm absorbance. Illustration done using Biorender.com

4.10.3. Caspase 3/7 apoptotic assay

To analysis apoptotic cells, Caspase 3/7 assay was performed on adult mouse cardiac fibroblast and mouse embryonic fibroblast after 48 hours of adenovirus infection in the 96 well plate with fluorescence light protection. Apo-One Caspase 3/7 assay, reagent was added with 1:100 dilution and incubated with the cells for 4 hours and absorbance of the fluorescence was read at 570nm in Advision plate reader. And for control/Blank used cell medium without cells.

4.11. Collagen assay

Collagens have always been challenging to determine in-vitro samples due to the limited number of samples. Hence circle collagen assay was used to determine the amount of collagens excreted in the supernatant of the respective cell-treated medium. 1ml of the cell culture medium was taken, and isolation and concentration were performed, incubating overnight at 4°C in a pre-cooled water bath and, and next day continued with the manufacturer's protocol with concentrating the soluble collagen and washing with acid-salt solution (Figure 14). The colorimetric reading was taken at 570nm. The reference standard was used to determine the amount of collagen in the knockdown cells compared to control cells.

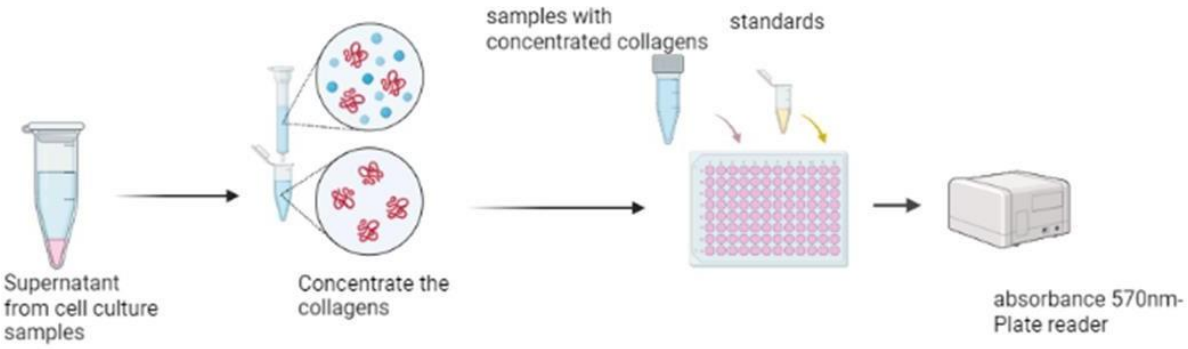

Figure 14: Scheme showing the isolation and measurement of soluble collagens using the manufacture's protocol.

Collagen assay was used to determine the amount of collagens excreted in the supernatant of the respective cell-treated medium. Concentrate the collagens with acid/salt-based mixture. Once the pellet of the collagen per sample can be obtained it was measured calorimetrically with 570nm absorbance and analysis was done with standard reference. *Illustration was used created using Biorender.com*.

4.12. Statistics

Statistical analysis and sample data analysis were performed with GraphPad Prism software, version 8. Data used for statistical analysis were represented as ± SEM (standard error of the mean). Each lane was considered a technical replicate for Western blot analysis, and for combined statistics, at least 3 biological replicates were performed (3 different cell isolations). All the statistics were done using an unpaired 2-tailed Student t-test comparing control versus knockdown groups in respective time points. Statistical significance was determined for p-value <0.05.

5. Results

5.1 Validation of eEF1A knockdown in cardiac fibroblast in mRNA level

eEF1A knockdown was performed in *in-vitro* models of adult mouse cardiac fibroblast (AMcFB) and mouse embryonic fibroblasts (MEF) by utilizing an adenovirus approach: adenovirus-cre and beta-Galactosidase (βgal) as control. RNA interference with siRNA targeting eEF1A1 and eEF1A2 were used in neonatal rat cardiac fibroblast (NRcFB).

5.1.1. Knockdown with siRNA in Neonatal rat cardiac fibroblast

NRcFBs were isolated and treated with sieEF1A1, sieEF1A2, sieEF1A1/A2 and siControl for 96 hours. During the first 72 hours, the cells were treated in 0.5%FCS medium and then placed into 10% FCS for the last 24 hours. The knockdown of eEF1A1 was measured by western blot and RT-qPCR. In the protein expression, eEF1A2 was unaltered indicated eEF1A1 to be the main isoform expressed in cardiac fibroblast (Figure15-A). The knockdown of eEF1A1 measured by RT-qPCR resulted in above 95% with both sieEF1A1 and sieEF1A1/A2 treatments, in which the results were normalized to siControl (Figure 15-B).

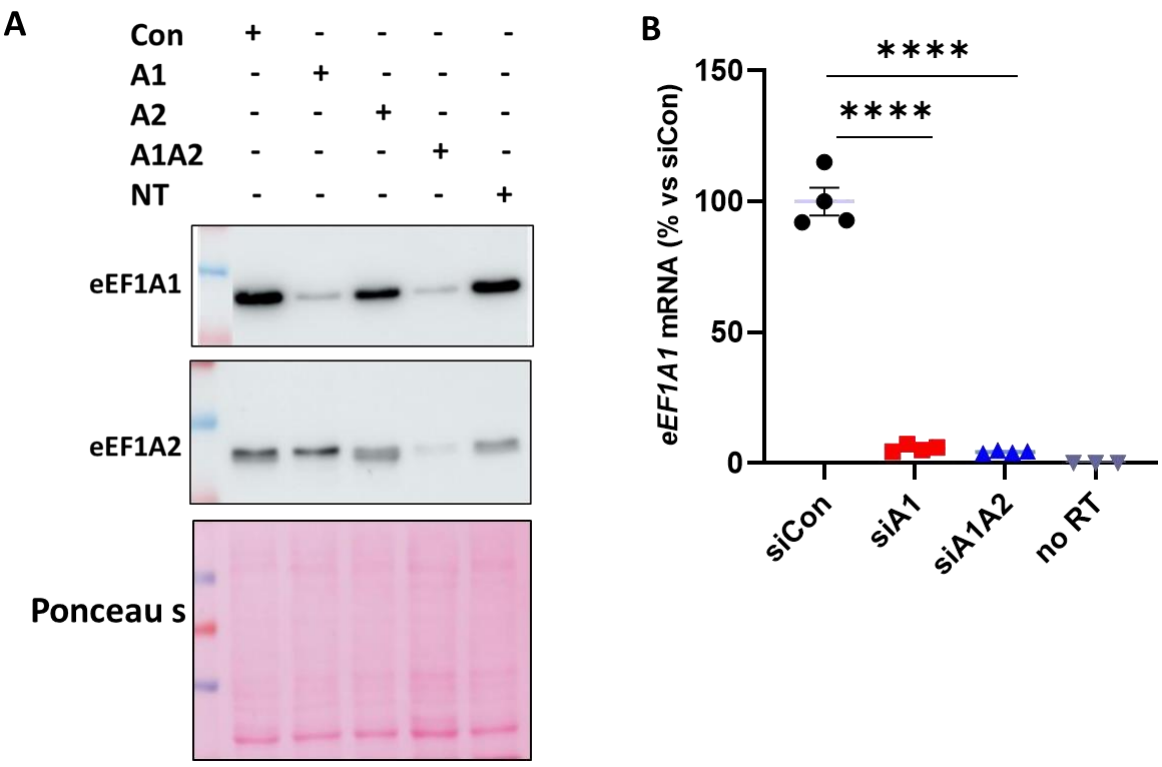

Figure 15: eEF1A1 shown to be the main isoform expressed in cardiac fibroblast and depletion of its expression in protein and mRNA level.

A: NRcFB treated with siRNA of eEF1A1, eEF1A2 and control. With western blot shown here the expression of eEF1A1 is depleted and eEF1A2 has no change in expression. **B**: shows NRcFB kd-eEF1A1 was measured using RT-qPCR and analyzed with respective controls which shows significant efficiency of downregulation of eEF1A1, eEF1A1A2. Each dot in respective conditions represent single cell isolation (n=4). Data was shown with mean ± SEM and the statistical significance determined with- p-value <0.05.

5.1.2. Knockdown with adenovirus in MEF and AMcFB

In MEF and AMcFB, eEF1A1 has been the main isoform having significant expression *in vitro* compared to eEF1A2. In this study, the eEF1A1/A2- flox/flox mice were chosen instead of eEF1A1 flox mice as eEF1A2 is present in very low level and might due to partial redundancy replacing eEF1A1 in parts. The downregulation of eEF1A was verified in mRNA level after infecting AMcFB and MEF cells with adenovirus Cre and βgal as control. For transfection of AMcFB (eEF1A1/A2- flox/flox mice, where the eEF1A1 and eEF1A2 alleles contained flox sites, enabling the ablation of eEF1A1 and eEF1A2 expression), the time-points for analyses in case of AMcFB were 24 hours and 48 hours, and for MEF cells (eEF1A1/A2- flox/flox mice) 24 hour,

48 hours and 96 hours. RNA was isolated at the end of indicated time-points and RT-qPCR was performed and a significant downregulation of eEF1A1 mRNA of 80% to 95% was detected in both models respectively (Figure 16).

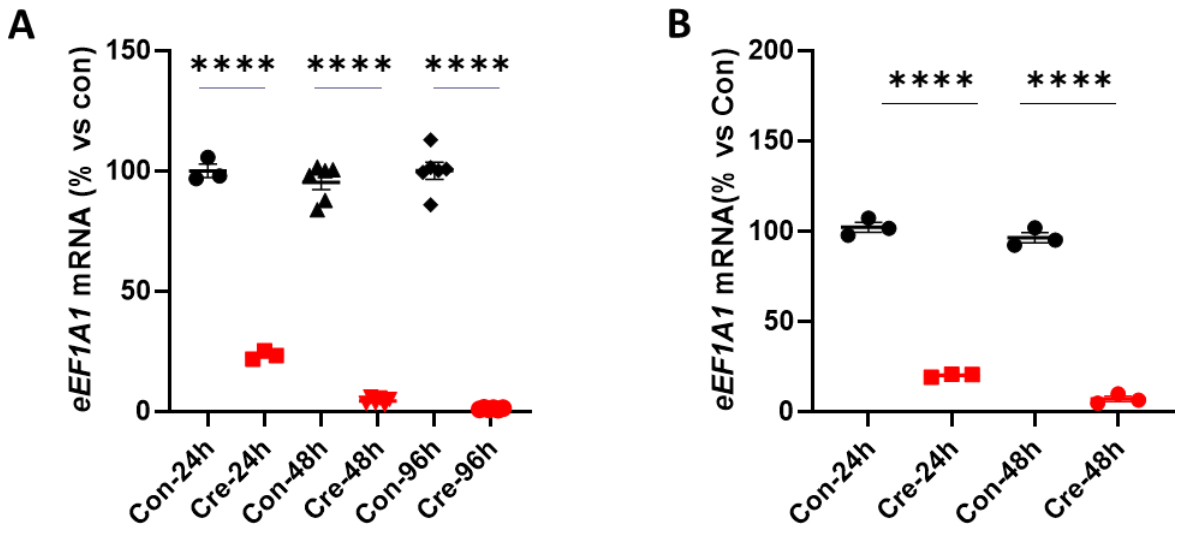

Figure 16:Knockdown of eEF1A1 at mRNA level in MEF and AMcFB
A: Knockdown of eEF1A1 in MEF at 24h, 48h and 96h. **B**: Knockdown of eEF1A1 in AMcFB at 24h and 48h. Each data points represent biological replicates, data shown are means of ± SEM and the statistical significance determined with *p-value <0.05 and ****p-value<0.0001.

5.2. Validation of eEF1A Knockdown in cardiac fibroblast in protein Level

5.2.1. Western blot to validate knockdown of eEF1A1 in NRcFB

The knock-down of eEF1A protein expression was investigated by Western blot. After 96 hours of RNA silencing, more than 50% downregulation of eEF1A1 and eEF1A1/A2 was evident compared to the siControl RNA (Figure 17-A). As shown in the previous results, similar outcome was obtained with eEF1A2 expression. Each sample represents biological replicates from different isolations of neonatal rat fibroblasts.

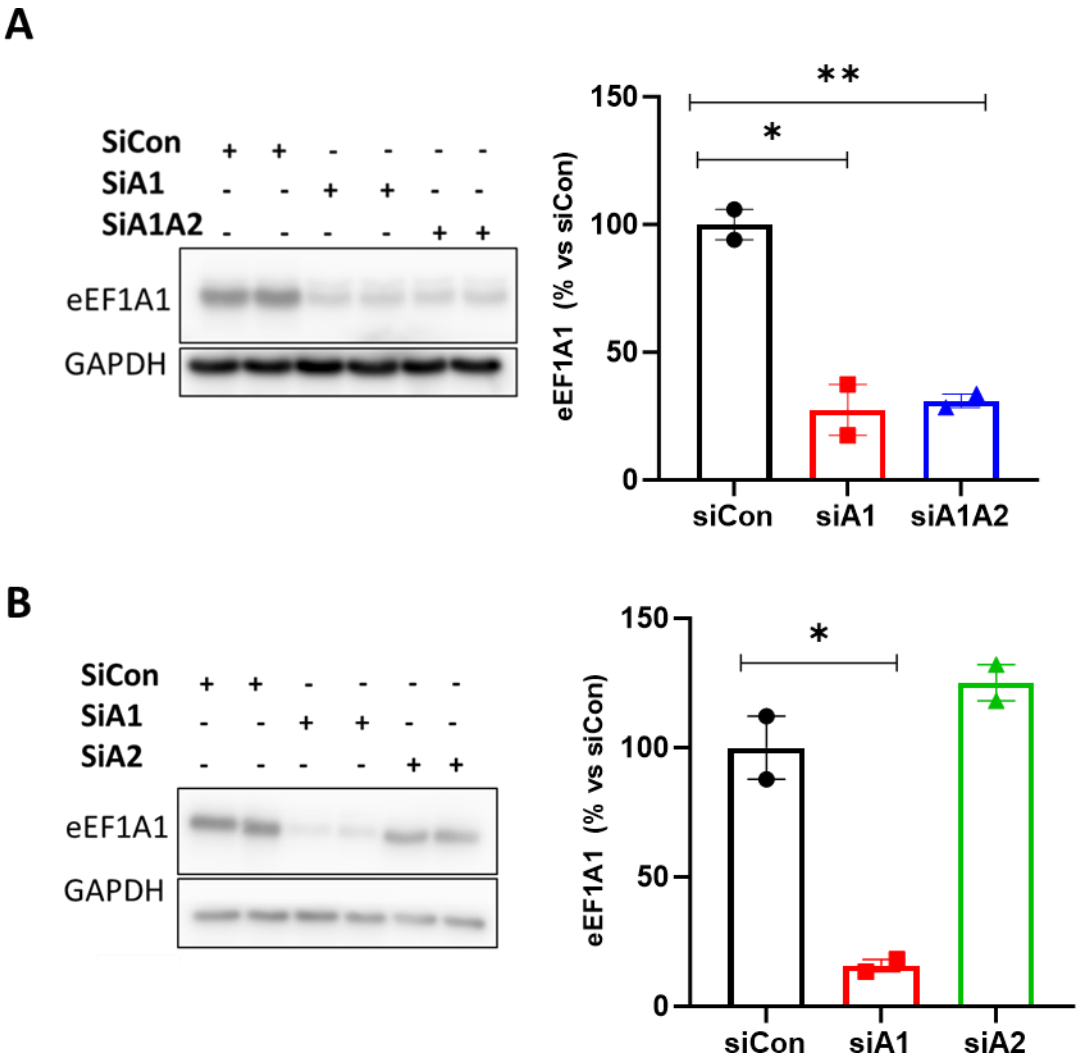

Figure 17: eEF1A1 knockdown in NRcFB at protein level.
A: Expression of eEF1A1 in protein level measured by western blot. **B**: Expression of eEF1A2 not altered measured with western blot normalized with respective control samples. Each data point represents biological replicates, data shown are means of ± SEM and the statistical significance determined with *p-value <0.05 and ****p-value<0.0001.

5.2.2. Validate knockdown of eEF1A1 in MEF and AMcFB

In MEFs, with time-points at 24 hours, 48 hours and 96 hours after infection protein analysis with Western blot revealed a consistent downregulation. Specifically, at 24 hours 50% knockdown was observed, while 48 hours treatment showed 60% and 96-hours treatment exhibited the maximum downregulation of 70% in comparison with their respective control

cells (Figure 18-A). In case of AMcFB, both 24 hours and 48 hours has shown a similar downregulation pattern (Figure 18-B). GAPDH was used for the normalization for all the samples.

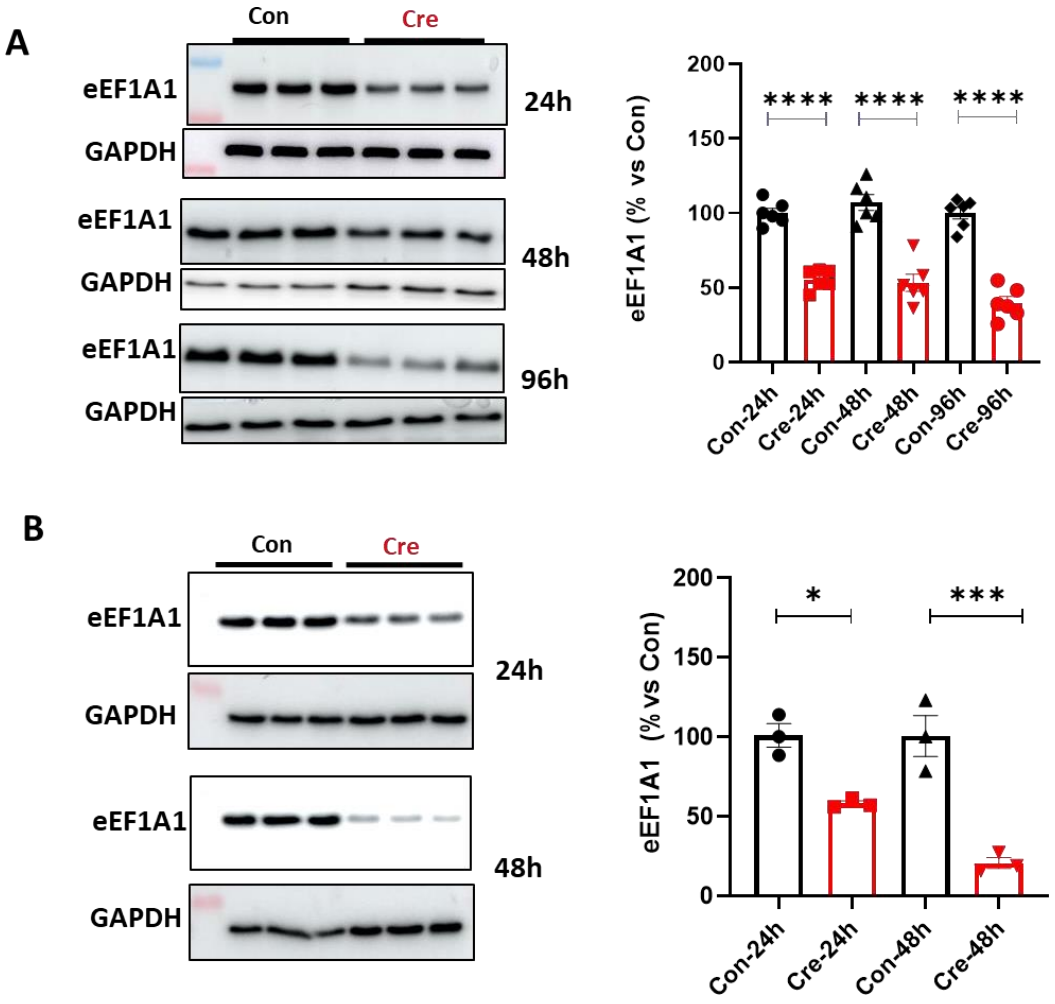

Figure 18: eEF1A1 knockdown in MEF and AMcFB with Western Blot

A: Knockdown of eEF1A1 (~50KD) in MEF at 24h, 48h and 96h normalized with GAPDH (37KD).

B: Knockdown of eEF1A1 in AMcFB at 24h and 48h normalized with GAPDH. Each data points represent biological replicates, data shown are means of ± SEM and the statistical significance determined with *p-value <0.05 and ****p-value<0.0001.

5.2.3. Adenovirus infection is not cytotoxic to MEFs

Since the knockdown of eEF1A1 in the protein levels was achieved with adenovirus Cre transduction, a toxicity test to eliminate doubts regarding false positive results was necessary. Hence, MEFs were isolated from wild type mice and with the same MOI and experiment strategy as the flox-MEFs was performed. There was no difference in the cell morphology as shown in Figure 19-A, and no change was detected when blotted for eEF1A1, in Cre treated cells and control cells (Figure 19-B).

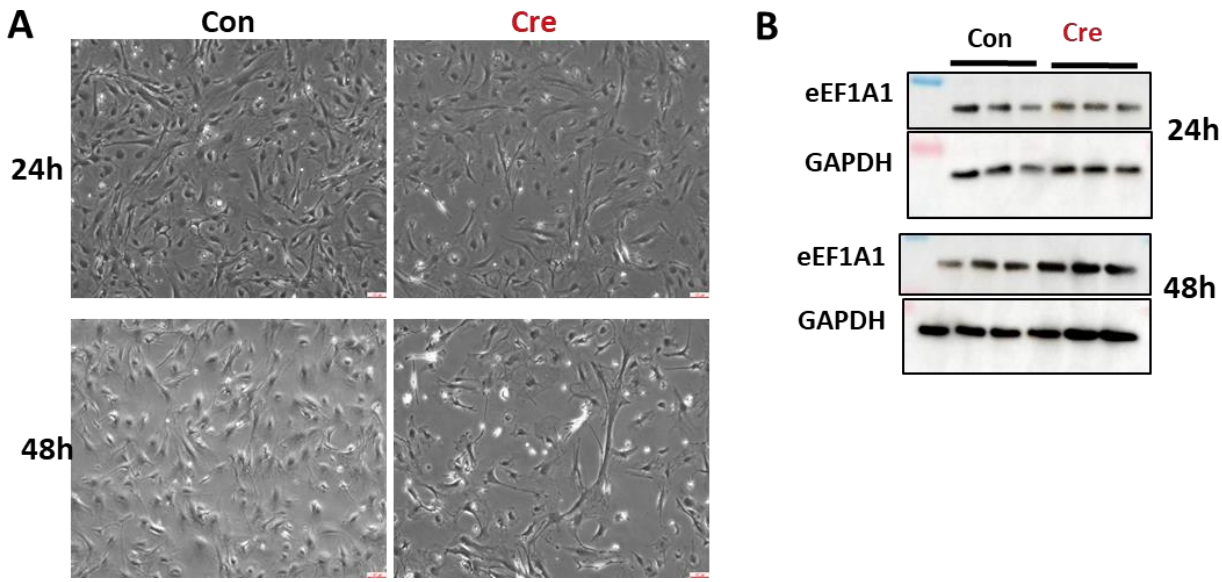

Figure 19: MEFs from WT mice to test the toxicity of Adenovirus treatment leading to unaltered eEF1A1 expression.
A: Images post adenovirus infection in MEFs-WT after 24 hours and 48 hours with respective control. **B**: Western blot for eEF1A1 expression measured indicated no Knockdown of eEF1A1 in MEF at 24h,48h normalized with GAPDH. Each data points represent biological replicates, data shown are means of ± SEM and the statistical significance determined with *p-value <0.05 and ****p-value<0.0001.

5.3. Immunofluorescence verification of the eEF1A1 knockdown in MEFs

Once the validation of eEF1A1 knockdown were obtained at the both protein and mRNA levels, immunofluorescence staining for the same protein revealed the visual observation of the selective and subsequent downregulation in individual cells. 24 hours post- knockdown (Figure 20) additionally provided a visual representation of the selective downregulation of eEF1A1. As depicted in the representative images, some cells still expressed the protein, while in others the expression was absent. Subsequently, the majority of cells showed no expression after 48 hours of downregulation.

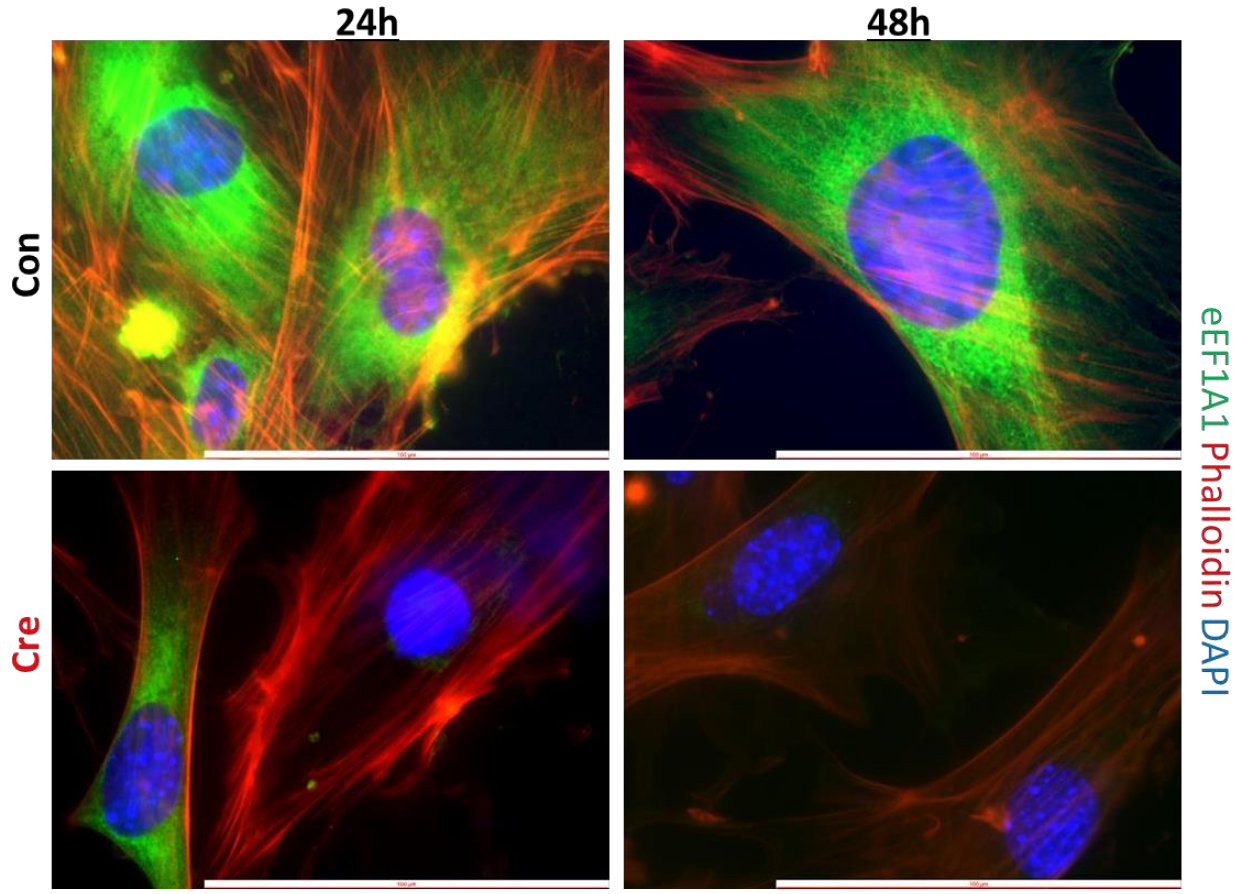

Figure 20: Immunostaining of eEF1A1 in MEF post 24h and 48h adeno-infection depicting knockdown of eEF1A1 in MEF at 24h and 48h.

5.4. The Assessment of Global Protein Synthesis with SUnSET Assay

As eEF1A is an essential protein that plays a significant role in the translation of proteins, further investigation was performed to measure global protein synthesis activity in the partial absence of eEF1A in cells. To validate the detection of newly synthesized protein, the puromycylation method, known as the SUnSET assay, was used.

The experimental setup was the same as previously described to validate the knockdown at the mRNA level.

Protein synthesis activity was significantly decreased in MEFs after 24 hours of eEF1A1 knockdown and gradually increased after 48 hours and 96 hours of knockdown of eEF1A1 (Figure 21-A). In AMcFBs, there was only a slight tendency in the 24 hours and a significant decrease in native synthesized proteins in 48 hours (Figure 21-B). Puromycin incorporation was normalized with GAPDH.

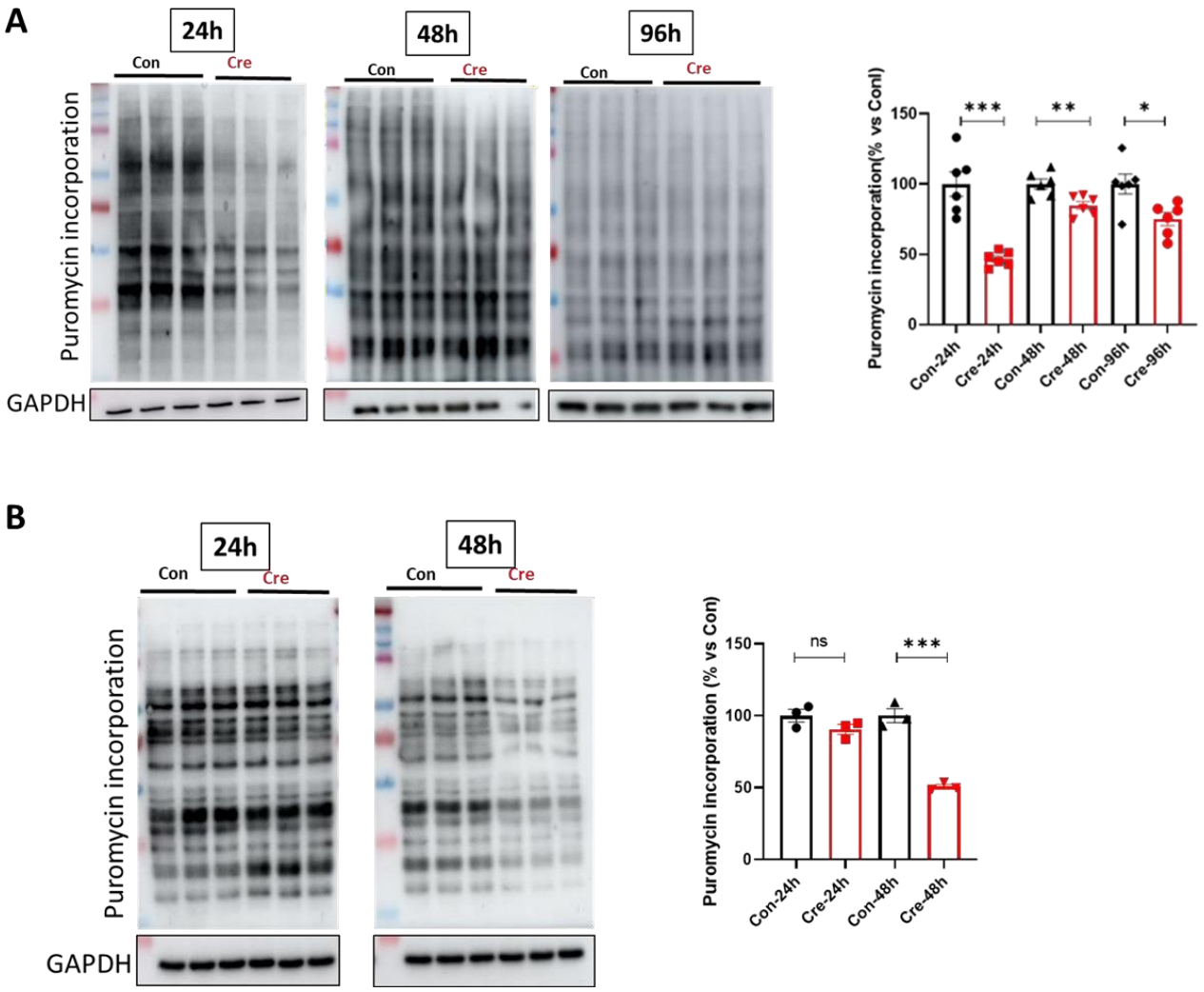

Figure 21:Global protein synthesis is reduced upon eEF1A knockdown

A: Puromycin incorporation demonstrated the attenuation of global protein synthesis upon the eEF1A1-KD in MEF at 24h,48h and 96h normalized with GAPDH. **B**: Puromycin incorporation representation of global protein synthesis expression reduced after eEF1A1-KD in AMcFB at 24h and 48h normalized with GAPDH. Each data points represent biological replicates, data shown are means of ± SEM and the statistical significance determined with *p-value <0.05 and ****p-value<0.0001.

5.5. Translational activity decelerated in Knockdown cells.

In this study, the expression of the global protein synthesis was clearly shown to be affected by eEF1A knockdown, confirming the canonical function of eEF1A. However, it has been more intriguing to examine whether the ribosomal activity is attenuated or not upon downregulation of eEF1A1.

In order to understand the ribosomal activity, polysome profiling was performed with harringtonine treatment. As described above, harringtonine is known for inhibiting the translation initiation. Therefore, this assay has been used to analyze the translational elongation speed by measuring the time of respective samples polysome profile after harringtonine treatment, which correlates with the translation elongation speed.

For this, MEFs were used to knockdown eEF1A for 48h; harringtonine was then subjected to the cells for 2min, 4mins, and no-harringtonine(0min) for both Kd-cells and control cells. The total mRNA peak, 80s peak, 60s, and 40s peaks followed by the polysomes were then analyzed per sample and revealed a deceleration of elongation speed in knockdown cells when compared to the respective controls, quantified with a ratio of total mRNA to polysomes (Figure 22).

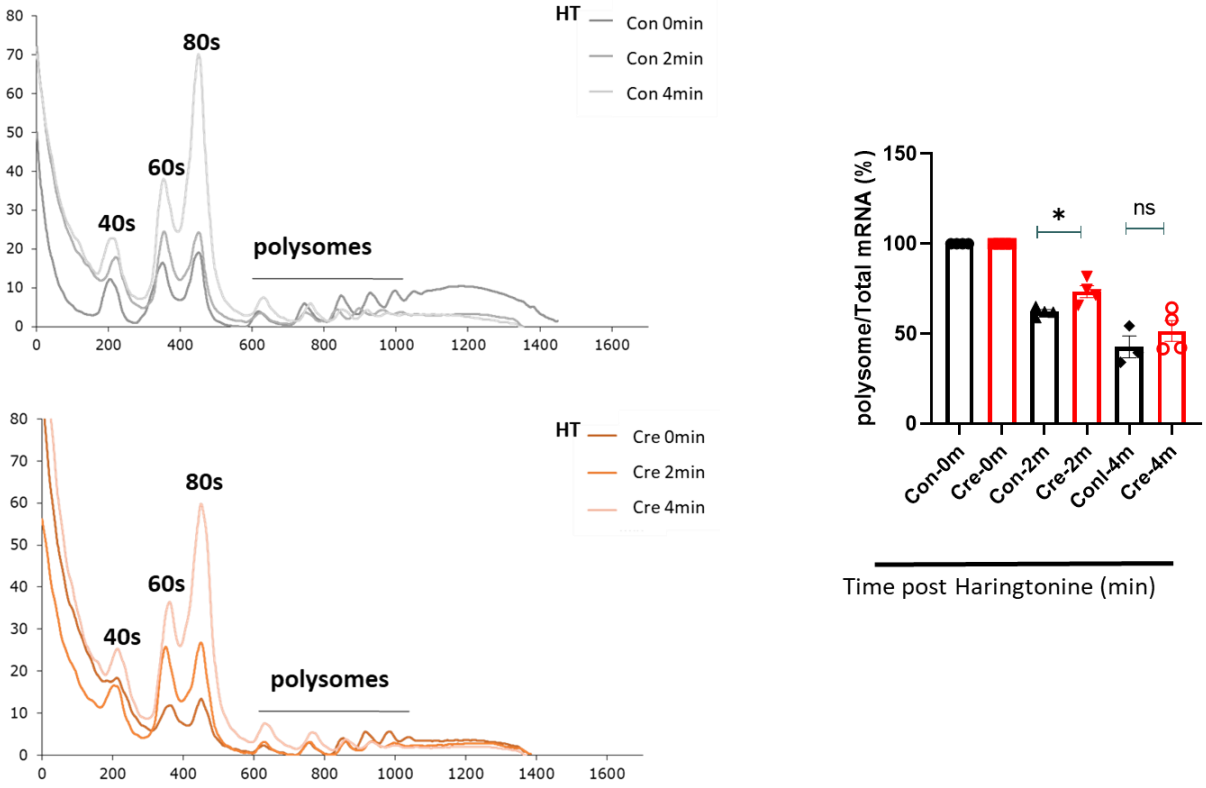

Figure 22:Polysome profiling with harringtonine suggest to have decelerated elongation speed in MEF-Knockdown cells.

Harringtonine is known for inhibiting the elongation initiation during translation. MEFs cells were treated with harringtonine for 0 min, 2 mins and 4 min. Later the cell lysate was measured in sucrose

gradient by giving the polysome profile showing the 40s,60s, 80s-monosomes and polysomes in peak-graph. The area between each of this peak is calculated which results in slow down of translational activity in kd-cells compared to the respective control cells. Each data point represents biological replicates, data shown are means of ± SEM and the statistical significance determined with *p-value <0.05 and ****p-value<0.0001.

5.6. Effect of eEF1A knockdown in Proteostasis Network

The proteostasis network is a system that maintains homeostasis in cellular processes. Given the observed reduction in global protein synthesis associated with eEF1A knock-down, it is also necessary to investigate potential collateral damage within the cellular process directly or indirectly linked to protein translation and degradation. Therefore, each component of the proteostasis system was analyzed in detail to analyze the effect.

5.6.1. Effect of eEF1A-knockdown on autophagy in MEFs and AMcFB

LC3b (tubule mediated-light chain 3b) and p62 are well-known markers for autophagosomal biogenesis. Proteins were isolated with the respective experimental setup for MEFs and AMcFBs, western blot was performed to identify the changes caused in the autophagy markers with the knockdown of eEF1A. Figure 23- A and B show the strong upregulation of LC3b and p62 activity in MEFs. Whereas, in AMcFBs a significant increase in LC3b activity in both the timepoints was shown and changes in p62 expression were not significant (Figure 23- C and D).

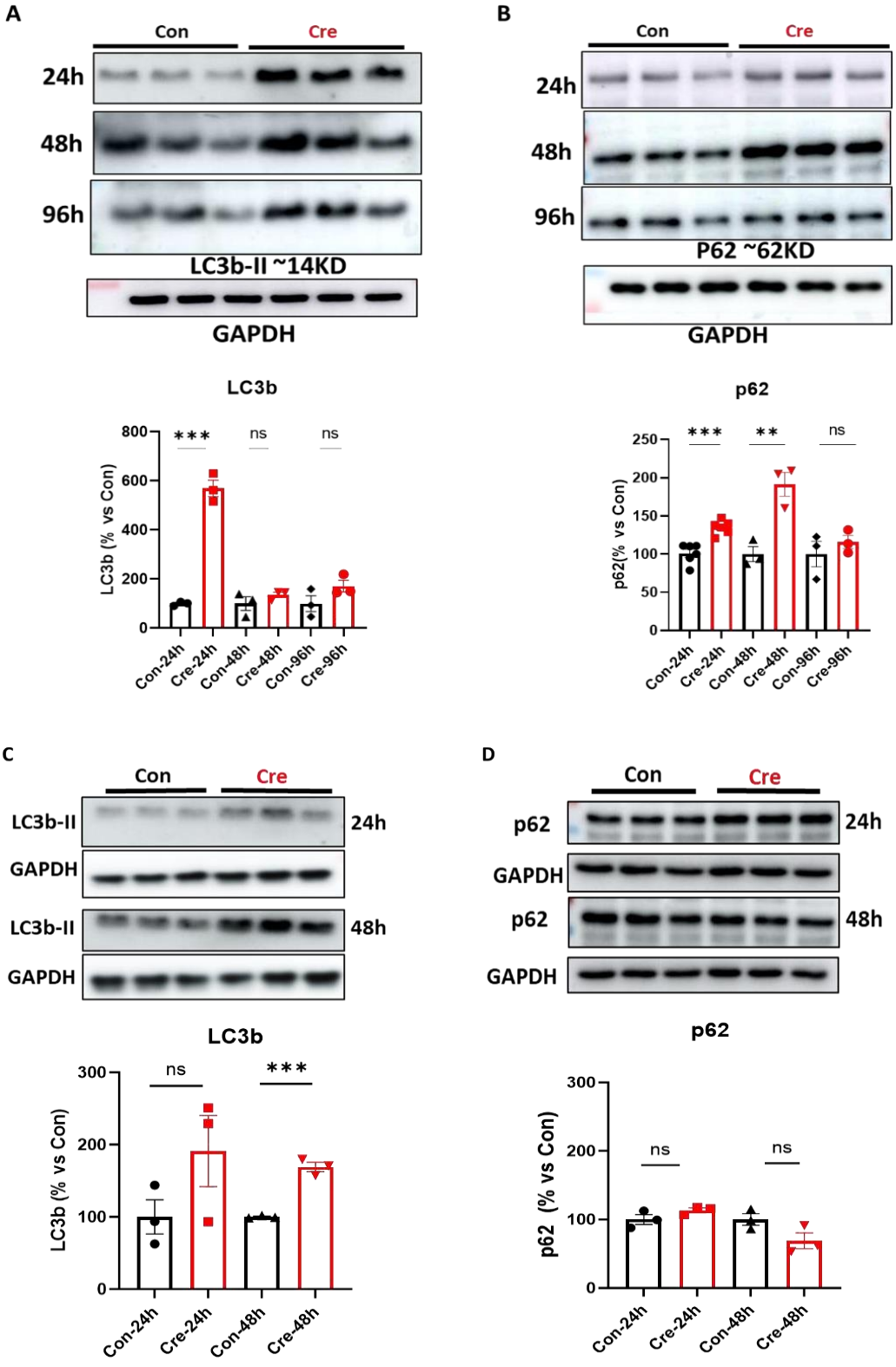

Figure 23:Autophagy is effected in eEF1A- Knockdown cells in MEF and AMcFB.

A: LC3b expression in MEF at 24h,48h and 96h normalized with GAPDH. **B**: p62 expression in MEF at 24h,48h and 96h normalized with GAPDH. **C**: LC3b in AMcFB at 24h and 48h normalized with GAPDH. **D**: p62 expression in AMcFB at 24h and 48h normalized with GAPDH. Each data points represent biological replicates(n=3), data shown are means of ± SEM and the statistical significance determined with *p-value <0.05 and ****p-value<0.0001.

5.6.2. Depletion of eEF1A1 alters the expression UPR genes

Another major aspect of the proteostasis network is unfolded proteins, which has been well studied and stated as one of the major malfunctions for causing some of the major diseases such as Alzheimer's disease[56]. In this study, given eEF1A's pivotal role in translation, there is a gap in the literature addressing its involvement in the Unfolded protein response (UPR): The UPR plays a key role in many aspects of the downstream and upstream activity of ER (endoplasmic reticulum) stress response. This study investigated the expression of specific genes and proteins (*CHOP*, *PUMA* and Transforming growth factor (*TGFβ)-2/3*) to comprehend the depth of eEF1A involvement in this pathway. Based on mRNA level analysis, the most prominent and consistent results seen in both models using MEFs and AMcFBs, were obtained from expression of *CHOP*, which significantly increased in knockdown cells.

TGFβ-2/3 has been widely studied for its vital contribution to various aspects of UPR activity and its significant implications in many disease models, such as CVDs. Here, eEF1A knockdown in both MEFs and AMcFBs resulted in a substantial decrease in the *Tgfb2/3* expression (Figure 24- A and B).

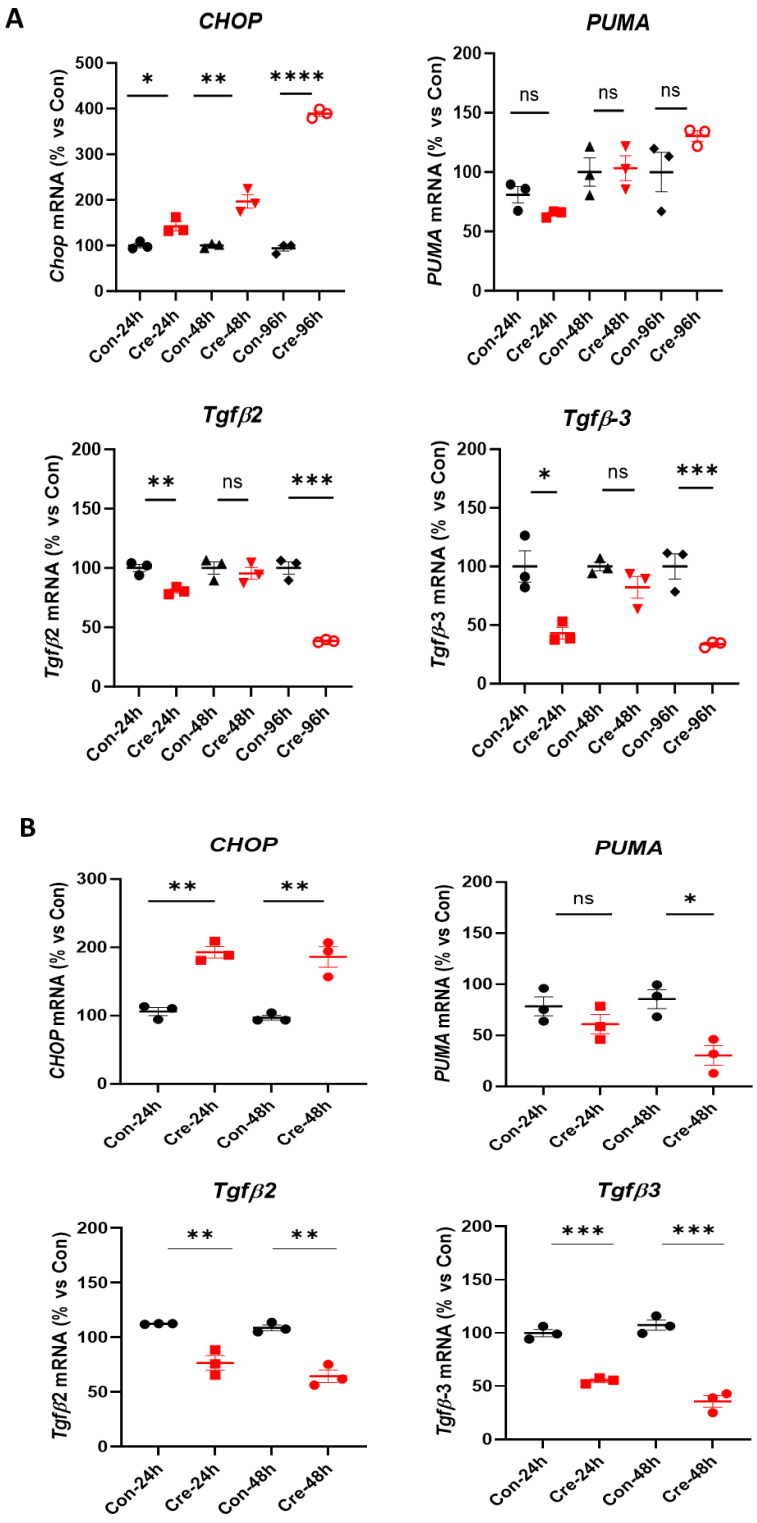

Figure 24: ER stress response genes modified due to depletion of eEF1A1 in MEF and AMcFB.
MEFs and AMcFB upon knockdown displayed significant modifications with the expression of selected ER-stress markers upon kd of eEF1A1 **A**: Shown here is the effect of eEf1A-knockdown in MEFs. **B:** A similar experimental setup for AMcFB showed overlapping results to MEFs in respect to the ER-stress markers expression with Kd cells. Each data point represents biological replicates (n=3), data shown are means of ± SEM and the statistical significance determined with *p-value <0.05 and ****p-value<0.0001.

5.7. Myofibroblast differentiation

Fibroblasts exhibit growth in size and can differentiate into myofibroblasts under mechanical stress. Myofibroblasts are morphologically distinct with higher stress fiber content and enhanced endoplasmic reticulum. Alpha-smooth muscle actin (αSMA) has become to be verified marker for myofibroblasts[57].

This study emphasizes fibroblast differentiation, clearly shown the reduced expression of αSMA in the knockdown cells. mRNA expression levels in all three timepoints for MEFs and two timepoints for AMcFB have indicated a significant downregulation of αSMA in knockdown cells compared to their respective control cells (Figure 25- **A** and **B**).

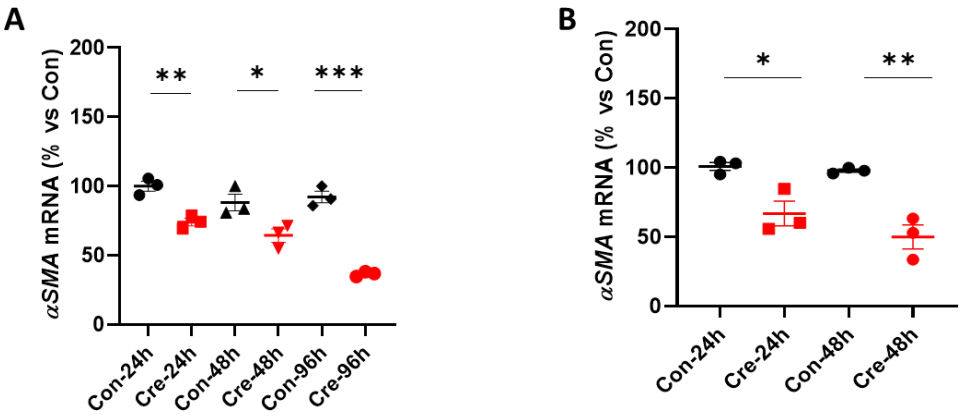

Figure 25: MEFs and AMcFB showed reduced mRNA expression of αSMA in eEF1A-KD cells
A: Shown to have decreased expression of the αSMA in KD- MEF cells in every time point. **B:** In AMcFB expression of the αSMA is shown to be reduced in KD cells. Validation by RT-qPCR each data points represent biological replicates (n=3), data shown are means of ± SEM and the statistical significance determined with *p-value <0.05 and ****p-value<0.0001.

Similarly, the protein expression of αSMA exhibited the same pattern of reduced expression in eEF1A knockdown cells. The highest significance was seen at 48-hours, and other time-points have shown the same tendency. The cells were collected from biological replicates and indicated as data points (Figure 26).

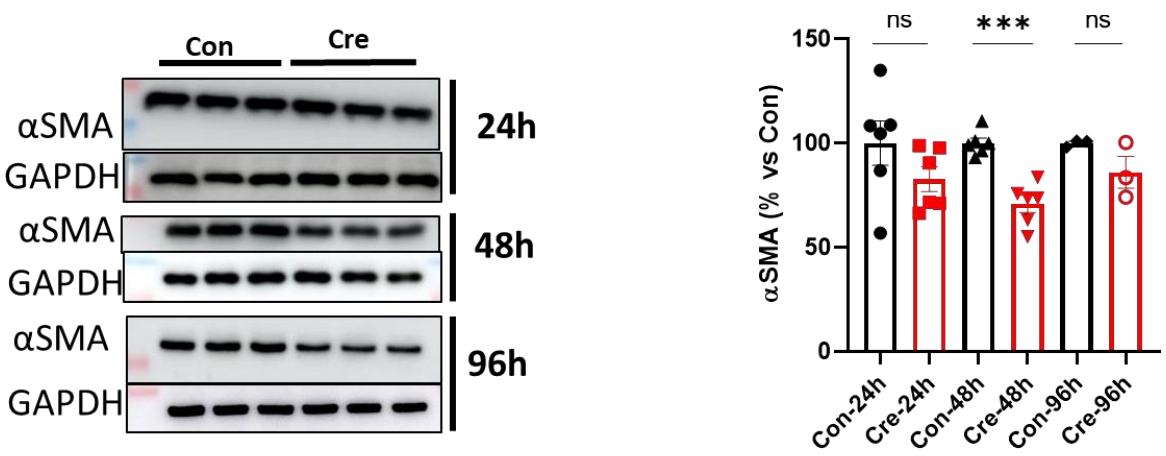

Figure *26:* Protein expression of αSMA reduced in MEFs upon eEF1A-KD

Western Blot shown at different timepoints (left side) and quantification of each timepoint respectively (right side) exhibiting the reduced expression of αSMA in eEF1A-KD cells, significant in 48h time point with other time point still showing the same tendency. Each data point represents biological replicates, data shown are means of ± SEM and the statistical significance determined with *p-value <0.05 and ****p-value<0.0001.

Further validation was also performed with immunofluorescence staining for the myofibroblast marker αSMA along with phalloidin, which is mainly staining the f-actin of the cells. Upon analyzing the images after 24 hours and 48 hours of Cre transduction in MEFs, in which 48 hours of treatment displayed significantly less fibroblast differentiation comparing to corresponding controls (Figure 27).

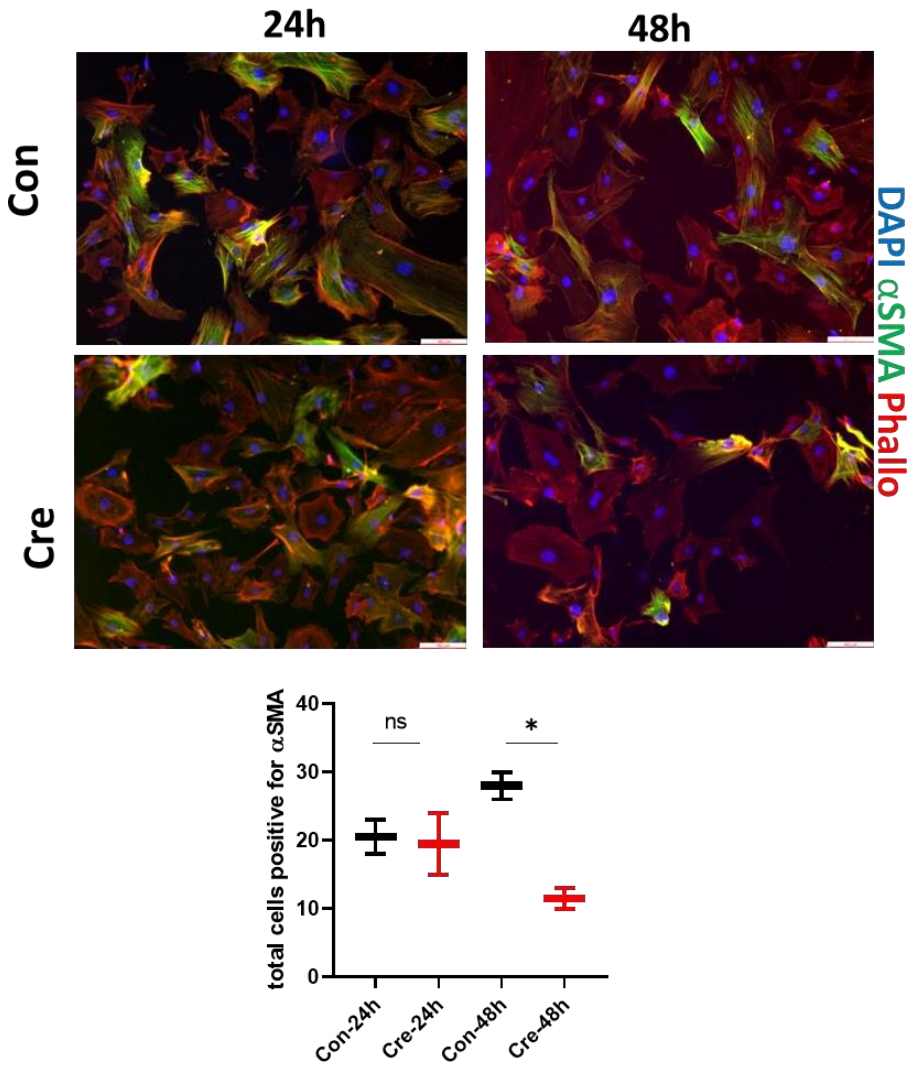

Figure 27: myofibroblast differentiation is reduced in the knockdown cells with immunofluorescence
Data points represent total number of cells per area, data shown are means of ± SEM and the statistical significance determined with *p-value <0.05 and ****p-value<0.0001.

Up to this point, the investigation in this study has given insight that eEF1A knockdown strongly influenced ER stress gene expression, reduced fibroblast differentiation, and increased autophagy activity.

5.8. Fibrotic genes modulated with knockdown of eEF1A

Fibroblasts are the major cell types in the heart that plays a crucial role in maintaining the productions of extracellular matrix and thereby helping to compensate any cardiac injury, aging or disease[58].

Expressions of the most common pro-fibrotic genes (*Col1a1, Col3a1* and *Fn1*) were examined in MEFs after adenovirus treatment at 24-, 48- and 96-hour intervals. MEFs were shown to have a depletion of mRNA expression in all the profibrotic genes in the knockdown cells (Figure 28: A).

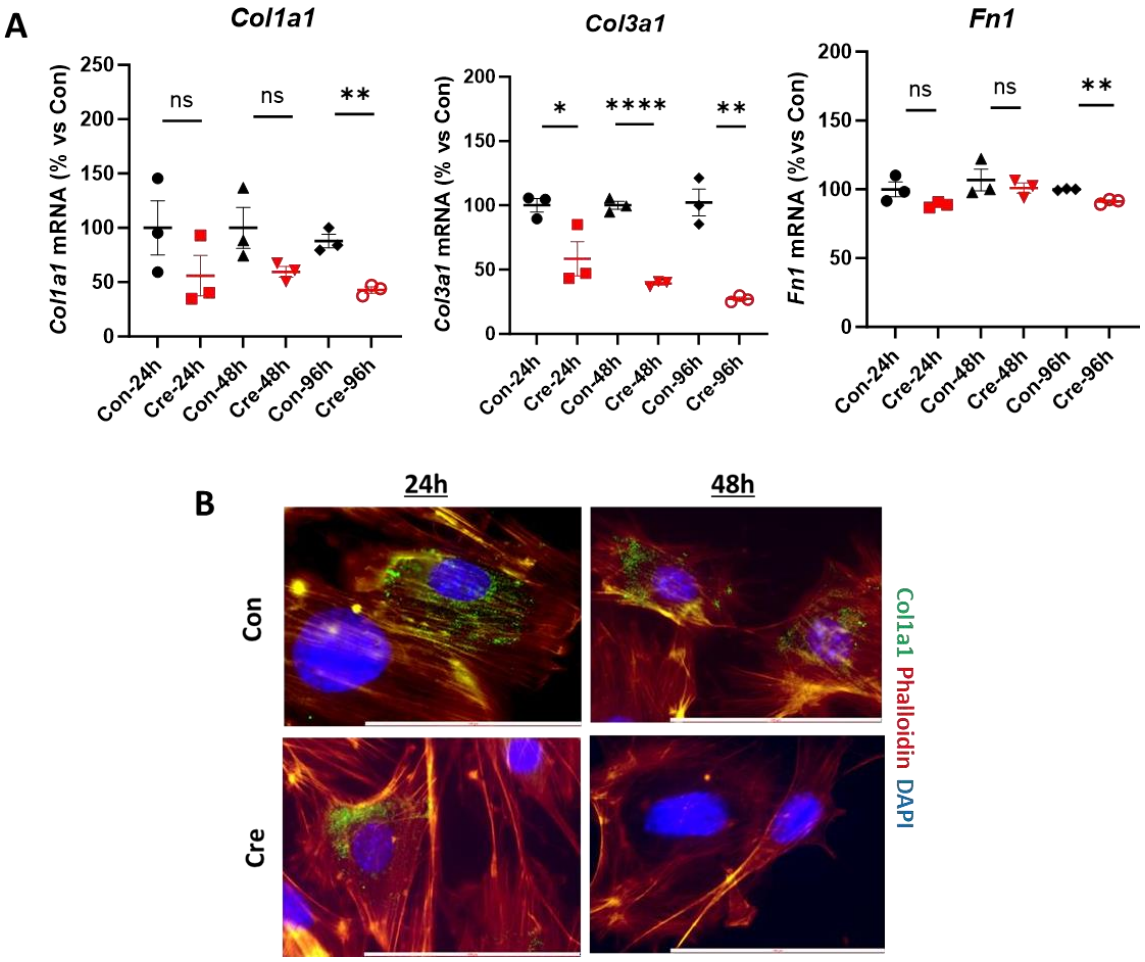

Figure 28: Effect on profibrotic genes post knockdown of eEF1A in MEFs

A mRNA expression of Collagens (*col1a1* and *col3a1*) and fibronectin reduced in eEF1A knockdown-cells. Each data point represents biological replicates, data shown are means of ± SEM and the statistical significance determined with *p-value <0.05 and ****p-value<0.0001. **B**: Col1a1 immunofluorescence staining with decreased localization in kd-cells.

The depletion of collagen with the highest effect observed at 48 hours shown in immunofluorescence, which correlated with mRNA results (Figure 28-B).

The fibrotic genes were also screened with AMcFB cells. Here, collagens (Col1a11 and Col3a1) and fibronectin have shown a significant downregulation in mRNA level of expression (Figure 29).

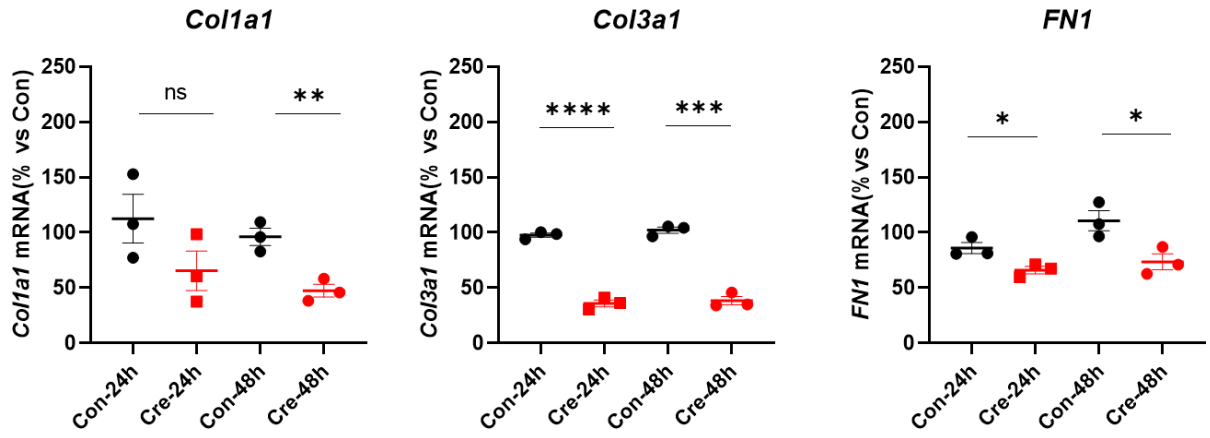

Figure 29: *Pro-fibrotic genes reduced with knockdown of eEF1A in AMcFB*
Post eEF1A1-knockdown in AMcFB exhibited mRNA expression of Collagens (col1a1 and col3a1) and fibronectin reduced. Each data point represents biological replicates, data shown are means of ± SEM and the statistical significance determined with *p-value <0.05 and ****p-value<0.0001.

Another optimal method to measure the amount of collagen released by the fibroblasts during remodeling would be direct measurement of produced collagen from the culture medium. Using a Sircol-soluble collagen kit, soluble collagens were isolated and concentrated before the measurement. Prior to collecting the supernatant from which the collagens are extracted and measured, the cell number was determined and used for normalization. Collagen assay also aligned with the results of reduced number of collagens exhibited by knockdown AMcFB

cells compared to the control cells (Figure 30). Standard references were also used quantifying the amount collagens.

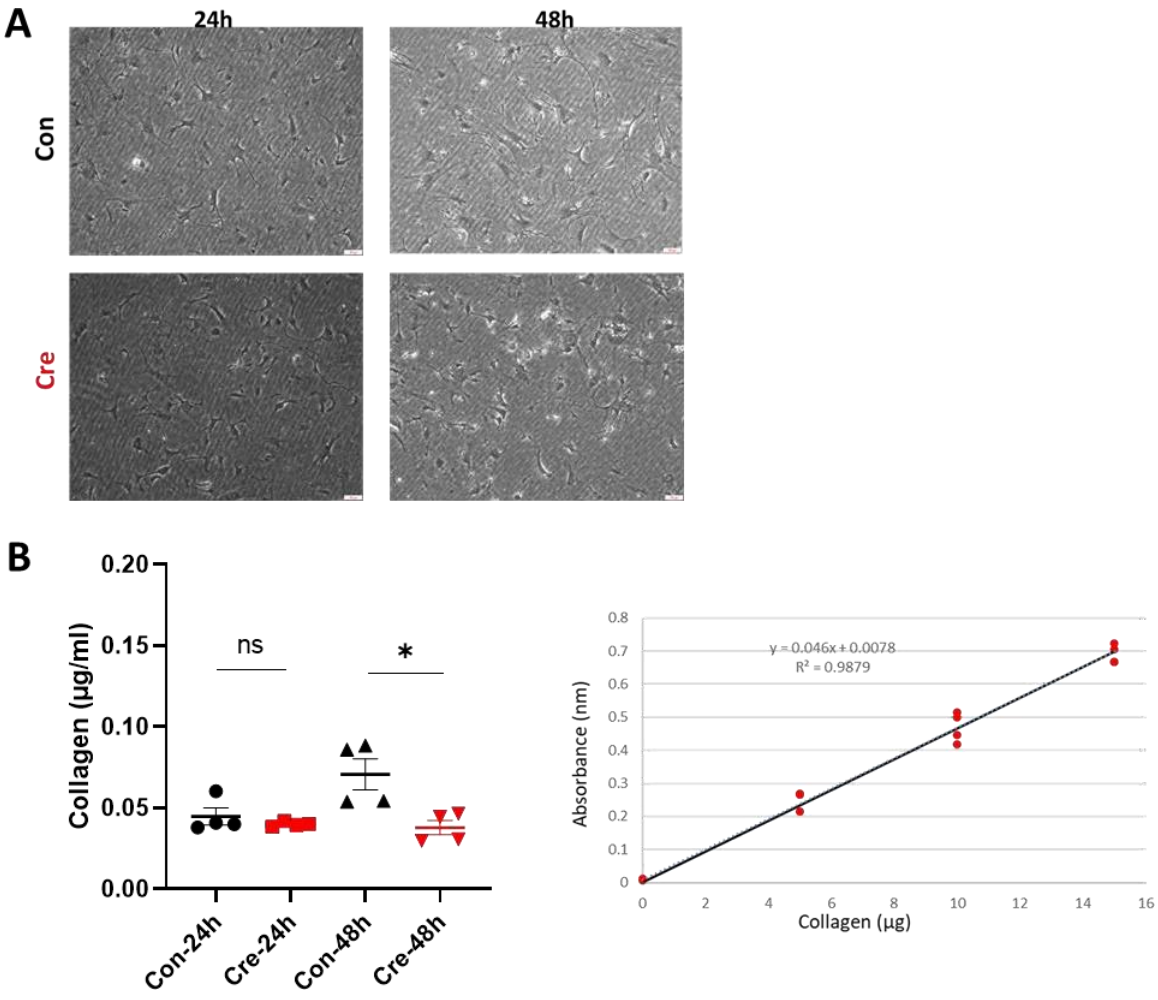

Figure 30:Collagen assay with AMcFB showing reduced expression in Kd cells.
A: Brightfield microscopy images of the cells post cre- infection both at selected timepoint 24h and 48h. **B**: Collagen assay result demonstrating reduced expression of soluble collagen in the supernatant of the medium collected post Cre-transduction at selected time points of 24h and 48h. Standard graph has been shown which was used for the analysis of the collagen amount in the experiment (right side). Each data points represent biological replicates, data shown are means of ± SEM and the statistical significance determined with *p-value <0.05 and ****p-value<0.0001.

5.9. Investigation of the effect of eEF1A with Functional Assays

Given the observed impact of eEF1A on puromycylation, autophagy and the ER stress response, a comprehensive understanding of its role in biological and cellular processes

requires a thorough characterization. Among the models used in this study, AMcFB has proven to be robust model. This was further validated with the functional assay done especially the apoptotic assay. Thus, *in-vitro* functional assays were performed; namely to elucidate cellular migration, proliferation and apoptosis.

5.9.1. Migration Assay

Migration assay was performed in all three cellular models, NRcFB, MEFs and AMcFB, as described in the methods section. Here in Figure 31, a slower wound closure compared to the control cells was observed within 24 hours. These results indicated the decline of the fibroblasts migration rate, which is one of the important functions of fibroblast upon activation.

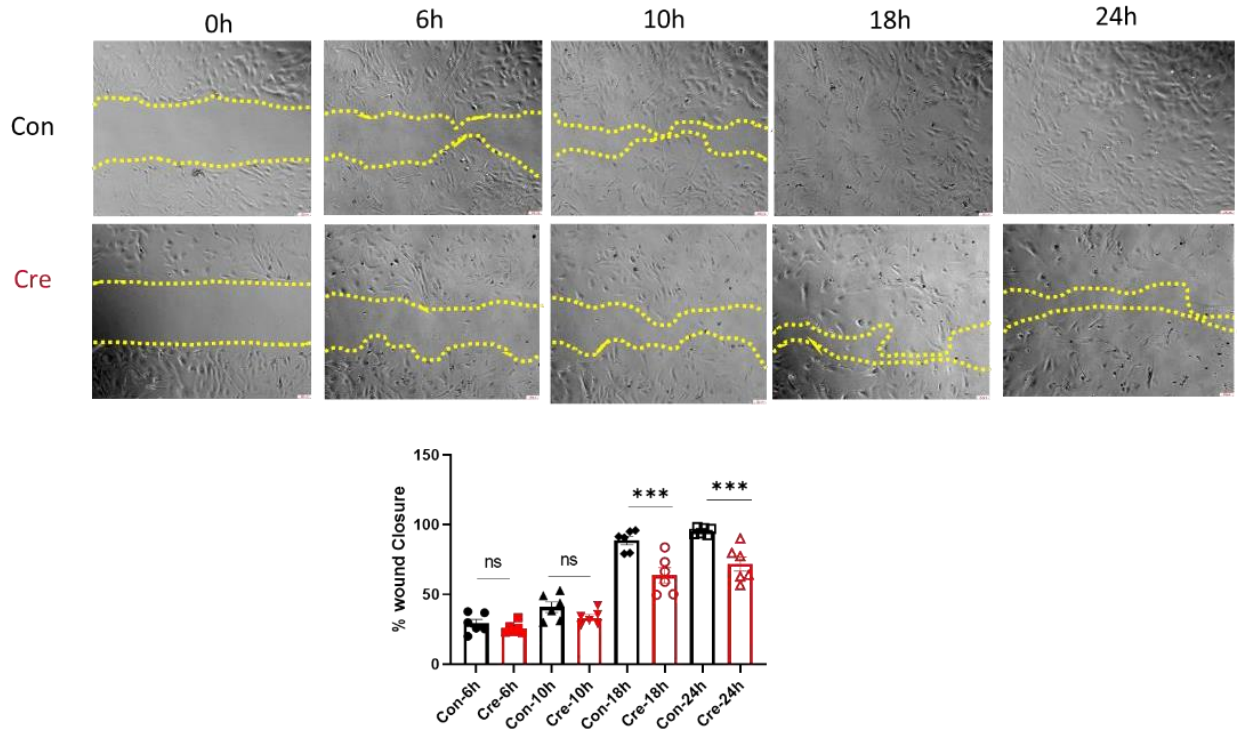

Figure 31: MEFs migration assay showing the delay in migration in knockdown cells.
Brightfield microscopy images shown the migration of the MEFs, with the yellow dotted line defined to trace the position of the cell population. Below shown the analysis of the migration assay calculated with the area left between yellow lines for each image per condition. Each data points represent biological replicates(n=6), data shown are means of ± SEM and the statistical significance determined with *p-value <0.05 and ****p-value<0.0001.

Similar experimental strategies were used with AMcFB and NRcFB. Mitomycin C, a proliferation inhibitor, was included in each treatment for both cell models. This treatment served as an additional control to eliminate the possibility that highly proliferative fibroblasts masking the actual observations in proliferation. In Figure 32 clearly indicated that fibroblasts isolated from both adult mouse heart and neonatal rat heart shown to have significant slower migration with and without mitomycin C.

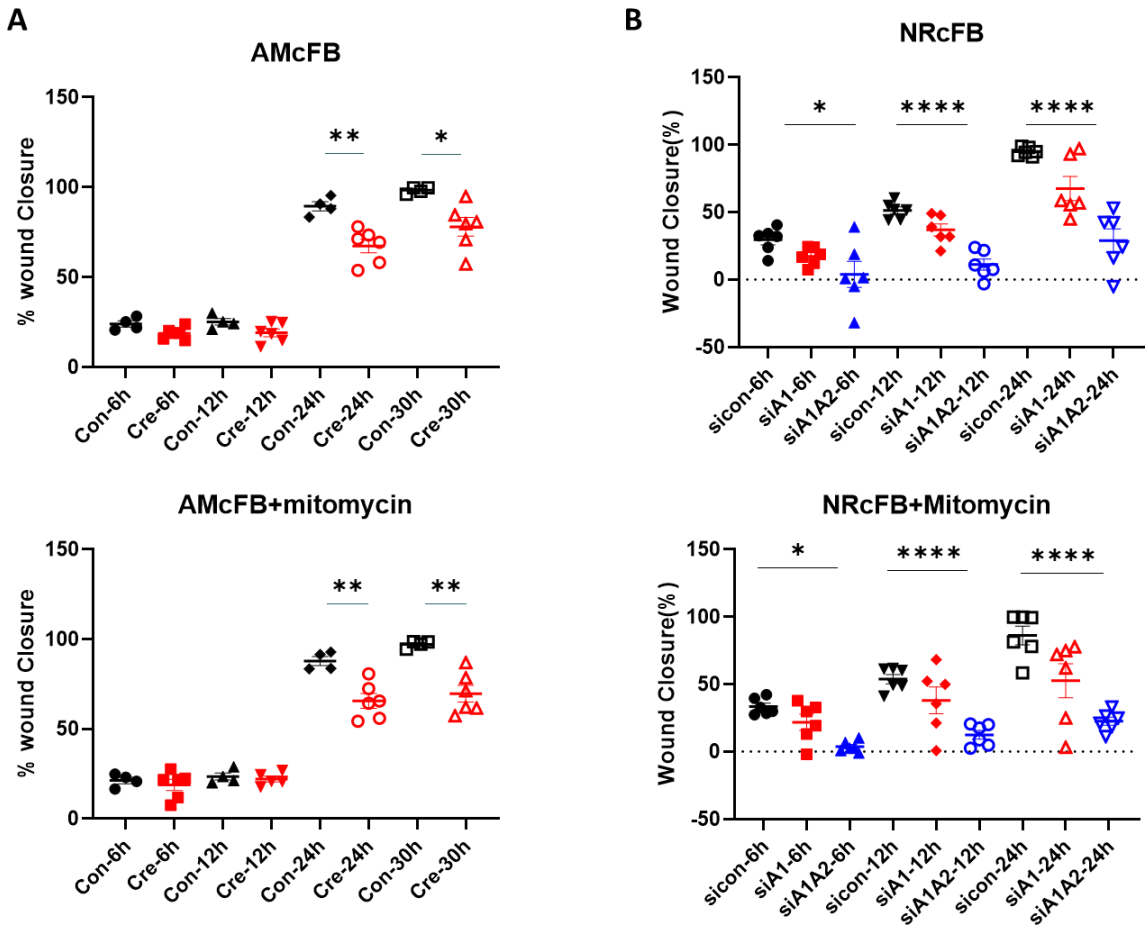

Figure 32: Migration inhibition also seen in AMcFB (A) and NRcFB (B).
Migration assay with control, using mitomycin C in both cell type. **A:** Validation of the AMcFB shown to have slow migration significantly in comparison to the respective control. **B**: Results of NRcFB has been consistent with the AMcFBs, shown to have reduced migration in Kd cells compared to control cells. Each data points represent biological replicates, data shown are means of ± SEM and the statistical significance determined with *p-value <0.05 and ****p-value<0.0001.

5.9.2. Proliferation shown to be inhibited with eEF1A1-knockdown cells.

Proliferation is an important aspects of fibroblast activation, during cardiac stress for example myocardial infarction or pressure overload[58]. Measurement of BrdU incorporation is a widely used quantitative method to determine proliferative cells. BrdU was added overnight onto the cells. Upon colorimetric detection, the knockdown cells were shown to have significantly fewer proliferating cells compared to the control cells in both MEFs and AMcFBs, respectively (Figure 33- A and B).

PCNA (proliferating cell nuclear antigen, 29 kD) is a well-known marker for indicating proliferating cells. In eEF1A knockdown cells (Figure 33-C and D) a notably reduced proliferation was evident, especially 48 hours post-knockdown in MEFs. In AMcFBs, both time points also showed reduced proliferation levels of PCNA.

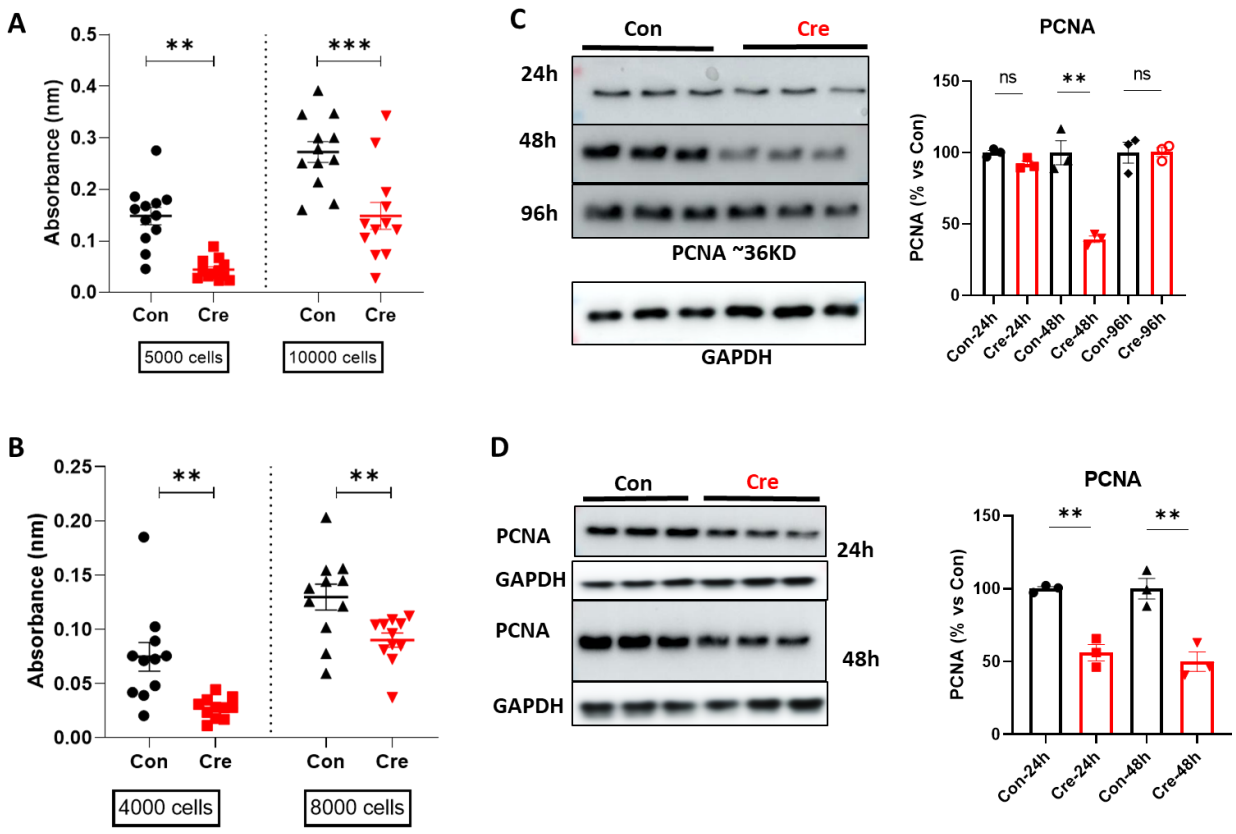

Figure 33: Proliferation of Knockdown cells are inhibited.

A: MEFs post 48hour knockdown in BrdU assay. **B**: AMcFBs post 48hour knockdown in BrdU assay. **C**: corresponds to PCNA of MEFs and **D**: represents data from AMcFBs of PCNA. Shown here in the blots of both the models is reduced expression of PCNA in knockdown cells. Each data points represent biological replicates, data shown are means of ± SEM and the statistical significance determined with *p-value <0.05 and ****p-value<0.0001.

5.9.3 eEF1A knockdown induce apoptosis in MEFs

Apoptosis is a programed cell death mechanism employed by cells to eliminate damaged or aberrant cells with abnormal activity. This process is very crucial for maintenance of cellular homeostasis, in which cells can undergo self-destruction, without the requirement of external influence. Apoptosis is mediated by proteolytic enzymes called caspases. Caspases are always present in dormant state in all cells, gets activated only with a cleavage by another caspase[59].

To evaluate the apoptotic state of MEFs and AMcFB cells after knockdown of eEF1A, Caspase 3/7 assay was utilized (Figure 34- A and B). Wild type-MEFs were used to test the toxicity of the Cre-adenovirus, which clearly displayed non-significant results (Figure 34-C). Additionally, MEFs notably showed apoptotic influx in eEF1A knockdown cells compared to the control, whereas the opposite effect was observed in the AMcFBs. This also reiterates the reason of AMcFB shown to have robust intercellular activity compared to MEFs.

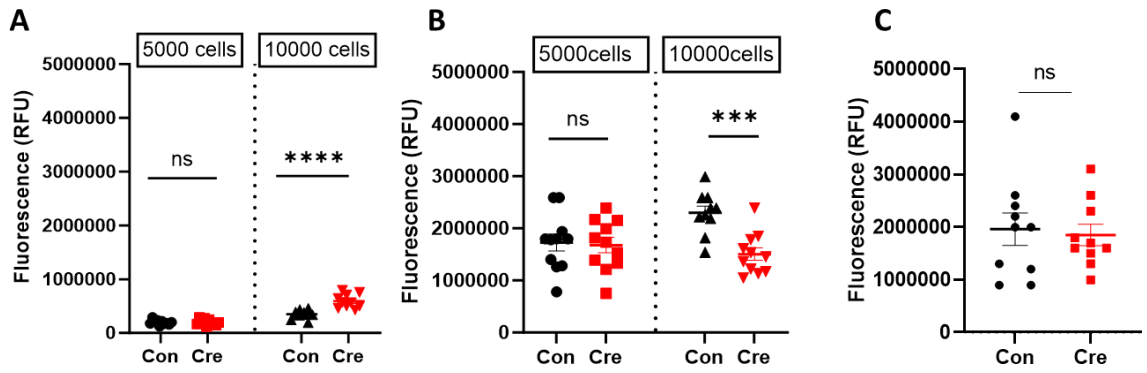

Figure 34: Depletion of eEF1A induce apoptosis in MEFs
A-MEFs are shown to be more apoptotic after the eEF1A-knockdown. **B**-AMcFB are less apoptotic after eEF1A knockdown. **C**-MEF-WT shown as a control apoptosis between Cre treated cell to control cells. Each data points represent technical replicates, data shown are means of ± SEM and the statistical significance determined with *p-value <0.05 and ****p-value<0.0001.

5.10. UPR modulates pro-fibrotic gene expressions

The unfolded protein response (UPR) pathways play a vital role in maintaining the homeostasis of cells. The ER stress is an adaptive reaction towards the activation downstream or upstream of the UPR. Three primary sensors, IRE (inositol requiring protein1), PERK (Protein kinase-like ER kinase), and ATF6 (Activating transcription factor 6), are involved in this complex signal transduction pathway orchestrating an adaptive response across the secretory pathway through transcriptional or non-transcriptional signals [29].

Given that the results of this study confirmed the significance of the UPR in the regulation of proteostasis upon eEF1A knockdown, a more thorough investigation into these listed pathways seeked to elucidate whether the downregulation of eEF1A triggered an adaptive response, or if this pathway functions concurrently with the elongation of translation system.

In this study, on the focus was directed towards one of the sensor pathways, namely PERK and it is downstream gene ATF4 (Activating Transcription Factor 4). By modulating the expression of these genes, the aim was to observe whether other pro-fibrotic or translational genes were affected.

5.10.1 Downregulation of PERK and downstream ATF4 genes in MEFs

To assess downregulation, WT MEFs were used for this experiment, where cells were seeded and treated with siControl, siEIF2AK3(PERK) and siATF4 for 48 hours in 0.5% fetal calf serum medium (Figure 35-A). Subsequently, the cells were lysed for RNA isolation for RT-qPCR validation, which revealed an almost 80% reduction in the expression of PERK and ATF4 (Figure 35-B).

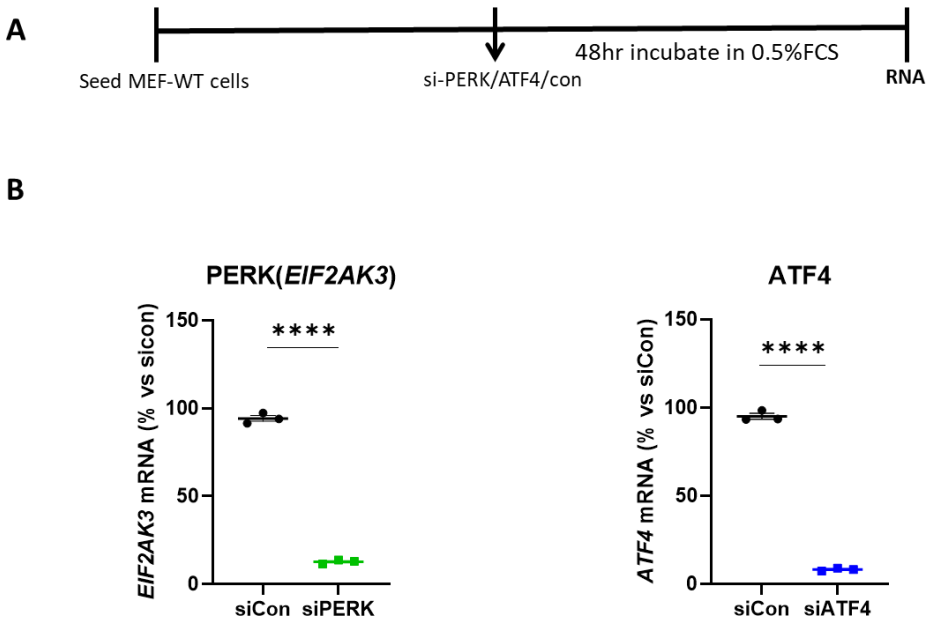

Figure 35: Validation of the downregulation of PERK and ATF4 in MEFs-wild type cells
A: Timetable of the experiment and treatments for the cells. **B**: Measurement of Knockdown of PERK and ATF4 in MEFs using RT-qPCR. After 48h of si-PERK treatment, the cells exhibited significant downregulation of PERK and ATF4 expression. Each data points represent technical replicates (n=3), data shown are means of ± SEM and the statistical significance determined with *p-value <0.05 and ****p-value<0.0001.

5.10.2. ATF4 mediated aberration the expression of the pro-fibrotic genes in eEF1A knockdown cells

In the previous results (Figure 28, 29), an apparent depletion of pro-fibrotic genes was observed in eEF1A1 knockdown cells in both MEFs and AMcFB. In order to validate the pro-fibrotic genes effect post eEF1A1-knockdown and UPR gene depletion, first verification of the knockdown of the target protein eEF1A1 was achieved after almost 80% reduction in mRNA levels (Figure 35). The mRNA expression of *PERK* and *ATF4* was depleted with almost 80% efficiency after 24 hours with the respective siRNA treatments.

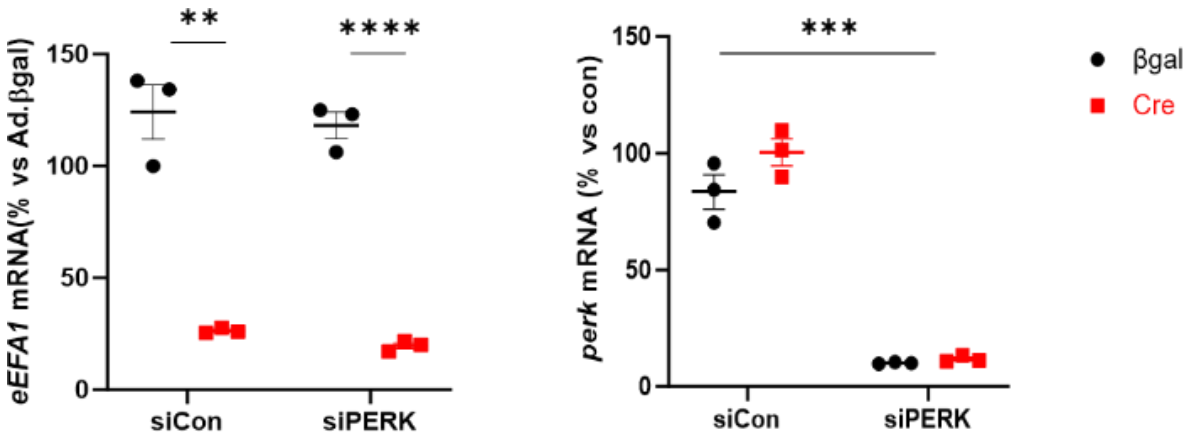

Figure 36: Validation of knockdown of *eEF1A1* and UPR sensor gene *(PERK)* expression
Measurement of the knockdown of eEF1A1 determined using qRT-PCR post 24h of virus transduction. The same cells were used validate the expression of PERK in knockdown cells along with appropriate control cells. Therefore, indicating the downregulation in siPERK treated cells in both control and Cre. Each data points represent technical replicates, data shown are means of ± SEM and the statistical significance determined with *p-value <0.05 and ****p-value<0.0001.

MEFs from the BL6-mice eEF1A1/A2-flox/flox were treated with siRNA for PERK(EIF2AK3) along with control for 24 hours (Figure 36). Screening of the pro-fibrotic genes using RT-qPCR, indicated a significant reduction in the expression of *Col3a1* in siPERK-AdCon vs AdCre in comparison to siControl-AdCon vs AdCre treated cells. A similar pattern was observed in *αSMA* and *Tgfβ3* not only in eEF1A-knockdown cells when compared with Con vs Cre. But importantly shown to have debilitated the pro-fibrotic genes further upon *PERK* downregulation shown the statistical significance in blue (Figure 37).

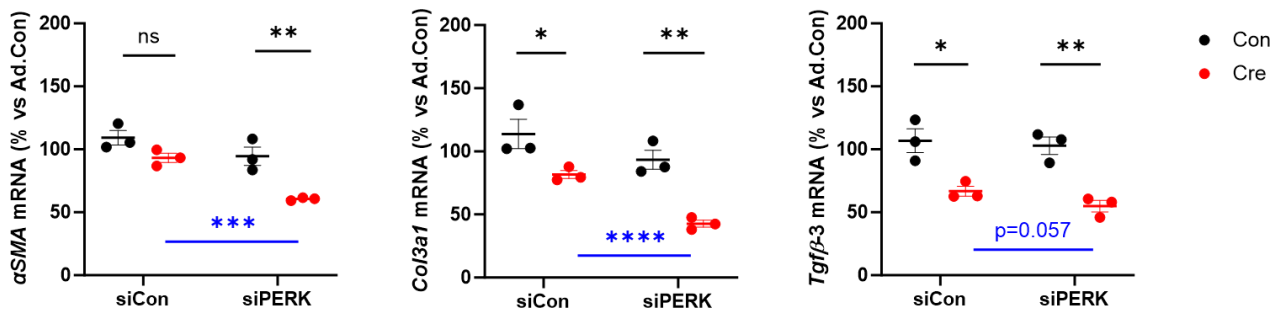

Figure 37: Pro-fibrotic genes expression debilitated upon siPERK in eEF1A knockdown MEF cells
With the same experimental setup of 24h of si-treatment and 24h of virus infection. Cells were measured using RT-qPCR to determine the selected pro-fibrotic genes downregulated in Cre-cells (black) also with PERK downregulated cells (blue). Each data points represent technical replicates, data shown are means of ± SEM and the statistical significance determined with *p-value <0.05 and ****p-value<0.0001.

The same experiment timetable was followed in AMcFB treatment. In AMcFB post transfection of siPERK and siATF4, the knockdown of eEF1A remained consistent to previous results. Also, significant downregulation of *PERK* and *ATF4* was displayed (Figure 38).

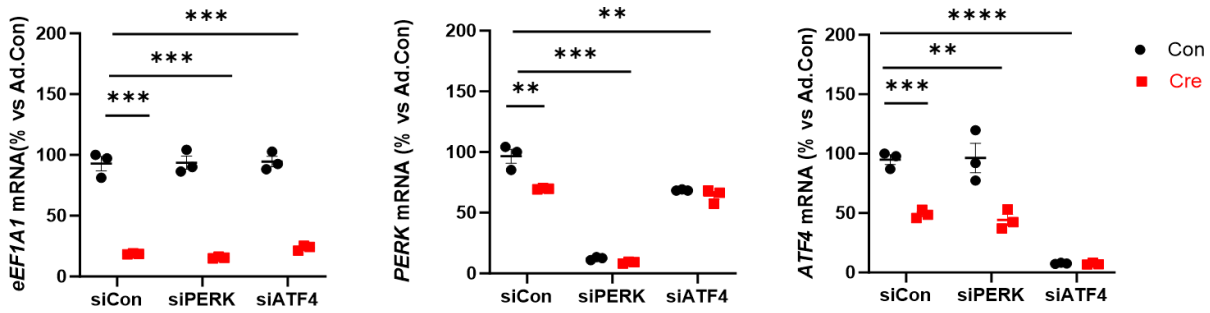

Figure 38: Validation of siPERK and siATF4 knockdown post kd-eEF1A in AMcFB cells
AMcFB cells are treated with siPERK, siATF4 and sicontrol for 24h, subsequently transduced each condition bgal and cre adenovirus to downregulate eEF1A1.The expression of each of these genes (*PERK, eEF1A1, ATF4*) was measured using RT-qPCR. Each data points represent technical replicates, data shown are means of ± SEM and the statistical significance determined with *p-value <0.05 and ****p-value<0.0001.

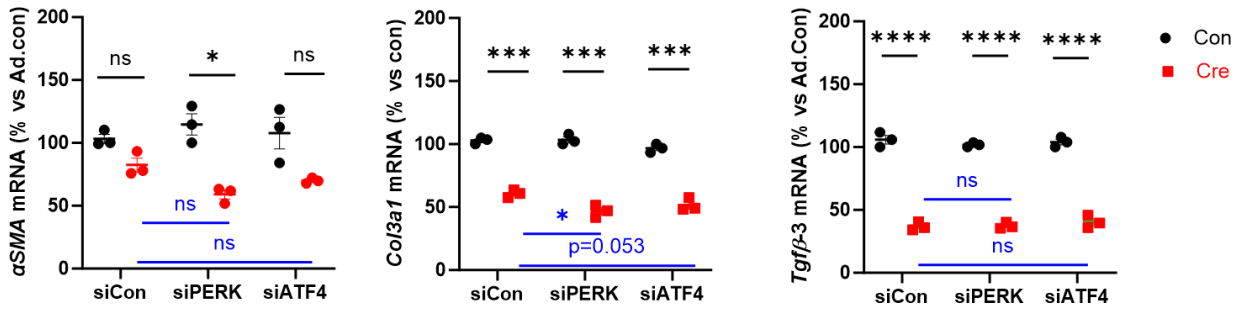

Figure 39: Effect of si-PERK and siATF4 on eEF1A1-kd AMcFB cells in pro-fibrotic genes.
AMcFB cells pos siRNA treatment of PERK, ATF4, control and KD of eEF1A1 with adenovirus transduction shown to have reduced pro-fibrotic gene expression. Cells with si-ATF4 along with Cre-treated condition demonstrates alleviated pro-fibrotic gene expression(black). Further debilitation of pro-fibrotic gene especially *Col3a1 shown with knockdown of eEF1A in siPERK transfected cells(blue).* Each data points represent technical replicates, data shown are means of ± SEM and the statistical significance determined with *p-value <0.05 and ****p-value<0.0001.

After validating the downregulation of PERK and ATF4 in eEF1A-knockdown AMcFBs, next was to investigate the treatments effect of pro-fibrotic genes. The effect of downregulation of PERK and ATF4 on pro-fibrotic genes in specific *Col3a1*, *αSMA* and *Tgfβ3* was assessed, and showed a significant downregulation in eEF1A1-knockdown cells, while only showing a tendency was observed for in *αSMA* with *ATF4* treated cells. (Figure39). Here the further aberration of *Col3a1* was seen in eEF1A-knockdown cells upon depletion of *PERK* (indicated as statistical significance in blue -Figure 39). These results insinuate the possible adaptive response of ER stress signals role when translation is attenuated.

6. Discussion

eEF1A is one of the crucial contributors to the translation elongation process, mediating tRNA transfer to the ribosomes [39, 49, 60]. The non-canonical function of eEF1A is less explored than its well-known canonical functions. However, in recent decades, the interest has shifted to its roles in subcellular processes, giving rise to new opportunities in the fields of cardiac hypertrophy, cancer and also in COVID-19 [52, 61-63].

This study focuses on elucidating the role of eEF1A in cardiac fibrosis using ex vivo cellular models to manipulate the expression levels of eEF1A, and subsequently investigating its functional effects on those cellular systems. Additionally, shown here, that counteracting eEF1A expression reduces general protein synthesis and triggers autophagy in fibroblasts, while predominantly reducing pro-fibrotic activity in these cells *in vitro*.

6.1. Knockdown of eEF1A1 works better on the mRNA than on the protein level.

In most cases, proteins are the primary regulators of the cellular processes, playing a crucial role in encoding the information stored in genomic DNA. The transcription of mRNA marks the initial step in protein translation, which is a pivotal process in for many cellular and molecular cascades [64]. This study found a much more efficient knock-down of eEF1A at the mRNA than at the protein level. It could well be that some of the eEF1A encoding pseudogenes become translated and thereby contribute to eEF1A protein in the eEF1A knock-down MEFs.

Pseudogenes are nonfunctional segments of DNA, which structurally resemble functional genes but lack the capability of protein-coding functions. Most pseudogenes arise from accumulation of mutations and can result superfluous copies of a gene which some might play

regulatory roles. While the EEFs (eukaryotic elongation factors) are well-studied coding genes, their pseudogenes have not been thoroughly explored.

Another possibility might be that eEF1A proteins might have an extremely long half-life. Studies have investigated the stability of eEF1A proteins [65]. The decay rate is comparable to another stable protein- GAPDH; however, it has been reported that the eEF1A may vary in different half-lives of mRNA but have comparable stability to corresponding proteins[65].

6.2. Regulation of protein synthesis and consequently translation activity is not completely ablated with the inhibition of eEF1A in vitro

eEF1A1, ubiquitously expressed protein in mammalian cells, is known to have a critical role in translating newly synthesized proteins. In this study, the knockdown of eEF1A1 has been shown to significantly, but incompletely affect the global protein synthesis in fibroblasts.

Protein synthesis was measured using puromycin incorporation, and a similar experimental setup was employed to measure the translation elongation speed with the harringtonine run-off assay. The translational activity is shown to be drastically affected by the depletion of eEF1A1 in fibroblasts (Figure 22). Numerous studies have provided evidence of translational activity being severely affected by the alterations in eEF1A1 expression in cells [56]. A key regulatory mechanism for translational control involves the phosphorylation of the α subunit of initiation factor 2 (eIF2α) at serine 51 [66]. GTP-bound eIF2 facilitates the delivery of initiator methionyl-tRNA (Met-tRNAi) as part of the 43S subunit complex, enabling initiation codon recognition and subsequent assembly of the fully active 80S ribosome at the start codon [67].

There is also a strong indication that phosphorylation of eIF2α increases with eEF1A1 knockdown, possibly compensating for the loss of function of the t-RNA delivery to the

ribosomes by eEF1A1 [68]. Further studies could therefore check eIF2α phosphorylation in the model shown in this study. It is also possible that protein synthesis is not affected by the downregulation of EEF1A itself, but by a proteostatic response in the model shown in this study. This notion is supported by studies suggesting that chronic mistranslation occurs, which then leads to a proteostatic response through triggering the ER-stress response, attenuating cytosolic protein synthesis and the cell cycle, while concurrently inducing the expression of chaperones and the ubiquitin-proteasome system to prevent the accumulation of misfolded proteins. Therefore, proteostatic activity appears to function as an adaptive response to ribosomal mistranslation. [69]. A proteostatic response is likely to contribute to reduced protein synthesis, supported by the finding in the models used in this study that showed ER-stress was elevated upon eEF1A knockdown.

6.3. Autophagy is shown to have a major effect upon eEF1A1-KD target cells

Autophagy is a mechanism associated with cell death, but also with the cell survival [70], which appears to be activated in response to disrupted translation activity by the depletion of eEF1A1. That is indicated by increased levels of LC3b, which is a common marker for autophagosome activity [71]. In this study, LC3b expression increased after eEF1A knockdown in all cellular models used (MEFs and AMcFB- Figure 23).

Aligning with the findings shown in this study, there have been publications [72-74] showing the strong correlation between autophagy and eEF1A1, which serves as a crucial target in the development of different chronic neurodegenerative diseases.

One of the prominent non-canonical function of the eEF1A1 is to play an essential role in regulating inflammatory diseases [75]. Mounting pieces of evidence indicate a correlation

between Alzheimer's pathophysiology and dysregulation of mammalian target of rapamycin complex 1 (mTORC1) signaling, where synthesis of eEF1A1 is regulated by mTORC1, proposing eEF1A1 as a master regulator in recruiting the transcription factors involved in the ubiquitination pathway to regulate the post-translation modification [76]. Lysosomes also engulf the cytoplasm mediated by chaperons, in order to pave the way for clearance of cytosolic proteins [77]. The mechanism involving the regulation of autophagic activity by eEF1A needs further investigation, but the data shown in this study might indicate that eEF1A1 promotes fibrotic activation by inhibiting autophagy.

6.4. Proliferation and apoptosis are attenuated in eEF1A1-KD cells

Apoptosis, a cellular process commonly known as programmed cell death, is observed in this study as a consequence of the depletion of eEF1A1 (Figure 34). During apoptosis, unwanted, harmful, or degraded cells are removed after protein degradation. The role of eEF1A1 in this process is not entirely novel; there have been studies [28, 29, 39, 77] suggesting the involvement of eEF1A1 in mediating protection from cell death.

Induction of the caspase-dependent apoptosis is associated with the Akt pathway (mainly Akt2 and Akt3)[78]. Synthesis of pro- and anti-survival processes are co-dependent on the cellular response upon up- or down-regulation of eEF1A1[73]. AMcFB has been the proven to be a robust in vitro model in this study which would be a good model for future pre-clinical studies, where the cells are not induced to programmed cell death upon alteration of eEF1A target protein. There have been differences in apoptosis *in the* models shown of eEF1A downregulation, which also clearly differs between MEFs and AMcFBs. Therefore, these results conclude that the impact of eEF1A on apoptosis might be less relevant for its profibrotic activity.

The association of eEF1A with cell proliferation is well-established, with studies demonstrating a correlation between the cell cycle rate and eEF1A activity [79]. As observed in this study, the proliferation rate is reduced in eEF1A1-knockdown cells (both in AMcFB and MEFs) (Figure 33). Moreover, overexpression of the eEF1A1/2 has shown exceeding influence in proliferating capacity in specific cell types in sub-optimal growth conditions [80]. It has been reported that cytoplasmic zinc finger protein 1 (ZPR1), when bound to eEF1A, restores the expected growth of proliferating cells, indicating the crucial role of eEF1A1 in cell cycle activity. The sub-localization of eEF1A in the cytoplasm and some parts of the nucleus has been shown in previous studies [81]. These different populations of eEF1A may contribute to the proliferating capacity during physiological conditions. Therefore, manipulations in the expression levels of eEF1A1 inhibits cell cycle progression, leading to the downregulation of fibroblast proliferation[39, 60, 81].

6.5. Downregulation of pro-fibrotic genes regulated the myofibroblast differentiation in eEF1A-KD models

During cardiac remodeling, the activation of fibroblasts to myofibroblast is the hallmark of fibrosis in many tissues, therefore providing a valuable target for potential therapeutic strategies [12]. In this investigation, abundant evidence showed that the pro-fibrotic genes are strongly downregulated by the depletion of eEF1A1 in AMcFB and MEFs (Figure 30). Many pro-fibrotic factors reported to have potential implications in the development of cardiac fibrosis, including angiotensin, endothelin, connective tissue growth factor, platelet-derived growth factor, and TGF-β1 [82, 83]. Additionally, TGFβ is noted to be playing a crucial role in the activation of myofibroblasts [84]. TGF-β-SMAD transduction pathways are pivotal for the development of fibrosis by regulating specific pro-fibro genic genes. Many fibrillar ECM

proteins, such as collagen and fibronectin, are also demonstrated to play an essential role in progressive fibrogenesis.[85, 86].

As shown in this study (Figure 25,26,27), αSMA expression has been consistently reduced in eEF1A1-kd cells at the mRNA, protein, and immunofluorescence levels. During cardiac fibrosis upon stimulation, the fibrotic response is triggered when circulating and myocardial pro-fibrotic growth factors and cytokines levels are elevated [10]. In the active phase, these pro-fibrotic growth factors and cytokines tend to bind to their receptors and then trigger the activation of signaling pathway and transcription factors, including SMADs, mitogen-activated protein kinases (MAPKs), protein kinase B (PKB, also called Akt1) and nuclear factor kappa B (NF-κB) [10, 87]. These pathological activations lead to the transformation of cardiac fibroblasts into myofibroblasts, which would express the highly contractile protein α-SMA, and produce a number of matrix metalloproteinases (MMPs) and tissue inhibitor of metalloproteinases (TIMPs) to regulate homeostasis of ECM. In cardiac fibroblast these pro-fibrotic transcriptional factors regulate the synthesis and secretion of pro-fibrotic growth factors and cytokines[87]. The secreted growth factors and cytokines by cardiac fibroblasts or other cells, for example, cardiomyocytes, endothelial cells and inflammatory cells, can function on cardiac fibroblasts or cardiomyocytes, forming a positive feedback loop and eventually amplifying the fibrotic response[10, 88]. Supporting these results, there have been many publications implying targeting anti-fibrotic genes for further pharmacological strategies could provide better understanding with mechano-stimulating pathways involved[89-91]. In this regard, counteracting eEF1A could be a valuable strategy.

6.6. UPR sensor genes shows a crucial conjecture in modulating pro-fibrotic genes in eEF1A1-KD cells

UPR is a molecular network that modulates the concentration of unfolded proteins as a response to stress in the ER. In order to reconstitute homeostasis, acts as a compensatory mechanism while cells upregulate chaperons and proteases to promote the degradation of misfolded proteins and facilitate protein folding[92]. There have been growing evidence showing that malfunction in the UPR system are involved in human diseases such as diabetes mellitus, atherosclerosis, Parkinson's disease [92, 93]. One of the three pathways involved in networking the UPR system is PERK (for pancreatic ER kinase or PKR-like ER kinase), a transmembrane protein whose N-terminal luminal domain is sensitive to the upstream ER stress signal, which C-terminal cytoplasmic domain facilitates eIF2α phosphorylation[33, 93, 94].

Many experimental studies have been focusing on role of eEF1A1 in cancer, chronic respiratory diseases, neurodegenerative disease by interacting with the UPR pathways [40, 54, 61, 95]. However, the molecular mechanism involving these interactions has not been elucidated. As shown in this study (Figure 37,38,39), the knockdown of eEF1A1 in siPERK and siATF4 treated fibroblasts has shown significant aberration in pro-fibrotic genes. There are assumptions that eEF1A1 modulates the pro-fibrotic genes via PERK sensory cell pathway[96].

In recent findings, inhibition of eEF1A1 by didemnin B has been shown to have beneficial effects on non-alcoholic fatty liver disease (NASH) [97]. The eEF1A1 inhibitor- didemnin B was shown to have moderately induced ER gene expression, which was similarly in this study, where *CHOP* mRNA level increased upon depletion of eEF1A1 in both MEFs and AMcFB. Didemnin B was demonstrated to lead to reduced inflammatory and fibrotic gene-expression,

posing a potential therapeutic target for the treatment of NAFLD upon partial inhibition of eEF1A1 [97].

Didemnin B binding blocks the translocation of the ribosomes by eEF2, thereby inhibiting protein synthesis [56, 97, 98]. Therefore, further investigation is needed to determine whether targeting eEF1A1 in fibrotic cell-type specific mouse models can counteract fibrosis. This can be achieved by treating the mice with an eEF1A1-inhibitor and analyzing the effects on different fibrotic diseases. Furthermore, novel pro-fibrotic effector molecules targeted by eEF1A1 could be identified by approaches such as Turbo-ID proximity labeling tagging[99]. Turbo ID proximity labeling of proteins using engineered biotin ligase to enable the labeling of interacting proteins in live cells *in vivo* to understand better how eEF1A mediates its pro-fibrotic effects[96, 99].

7. Conclusion and Outlook

In this study, eEF1A1 has shown to be involved in cardiac fibrosis which was demonstrated using different *in vitro* models MEFs, AMcFB and NRcFB.

In recent research studies, the roles of non-canonical functions of eEF1A1 have been topic of investigation especially in disease such a Parkinson's and cancer. There needs to be more understanding of the role of eEF1A1 in cardiac fibrosis, which is one of the most common pathological consequences of heart failure. The aim was to investigate whether downregulation of eEF1A in fibroblasts could reduce their pro-inflammatory activity and whether the canonical or the non-canonical function of eEF1A was involved.

Therefore, these results have been encouraging to understand further if eEF1A could be a good target for suppressing cardiac fibrosis, for example by using eEF1A inhibitors. One of them, Didemnin B, has been used widely by many researchers to investigate the role of eEF1A1 in liver fibrosis[97]. Treatment with Didemnin B has improved hepatic lipotoxicity in obese mice with NAFLD, indicating a potential therapeutic strategy [100]. eEF1A1 depleted cells impact the thermotolerance and debilitate the heat shock response. However, adjusting the transcriptional yield to translational needs improved heat shock response activity [95].

All of these data suggested that counteracting the expression of eEF1A1 in fibrotic mouse models such as the myocardial infarction or transverse aorta constriction should be conducted, in order to test, whether fibrosis can be ameliorated.

Further investigations into the molecular mechanisms underlying the anti-fibrotic effects associated with eEF1A1 suppression could also provide valuable insights into developing targeted therapies for cardiac fibrosis.

8. References

1. Bradshaw, P.T., et al., *Cardiovascular disease mortality among breast cancer survivors.* Epidemiology (Cambridge, Mass.), 2016. **27**(1): p. 6.
2. Olvera Lopez, E., B.D. Ballard, and A. Jan, *Cardiovascular Disease*, in *StatPearls*. 2023, StatPearls Publishing.
3. Tomasoni, D., et al., *Highlights in heart failure.* ESC Heart Failure, 2019. **6**(6): p. 1105-1127.
4. Tanai, E. and S. Frantz, *Pathophysiology of Heart Failure.* Comprehensive Physiology, 2015: p. 187-214.
5. Yancy, C.W., et al., *2013 ACCF/AHA guideline for the management of heart failure: a report of the American College of Cardiology Foundation/American Heart Association Task Force on Practice Guidelines.* J Am Coll Cardiol, 2013. **62**(16): p. e147-239.
6. Tan, L.B. and A.S. Hall, *Cardiac remodelling.* Br Heart J, 1994. **72**(4): p. 315-6.
7. Frantz, S., et al., *Left ventricular remodelling post-myocardial infarction: pathophysiology, imaging, and novel therapies.* Eur Heart J, 2022. **43**(27): p. 2549-2561.
8. Weber, K.T., *Targeting pathological remodeling: concepts of cardioprotection and reparation.* Circulation, 2000. **102**(12): p. 1342-5.
9. Segura, A.M., O.H. Frazier, and L.M. Buja, *Fibrosis and heart failure.* Heart Failure Reviews, 2014. **19**(2): p. 173-185.
10. Kong, P., P. Christia, and N.G. Frangogiannis, *The pathogenesis of cardiac fibrosis.* Cellular and Molecular Life Sciences, 2014. **71**(4): p. 549-574.
11. Weiskirchen, R., S. Weiskirchen, and F. Tacke, *Organ and tissue fibrosis: Molecular signals, cellular mechanisms and translational implications.* Molecular Aspects of Medicine, 2019. **65**: p. 2-15.
12. Larson, S.A., D.M. Dolivo, and T. Dominko, *Artesunate inhibits myofibroblast formation via induction of apoptosis and antagonism of pro-fibrotic gene expression in human dermal fibroblasts.* Cell Biology International, 2019. **43**(11): p. 1317-1322.

13. Zeisberg, M. and R. Kalluri, *Cellular Mechanisms of Tissue Fibrosis. 1. Common and organ-specific mechanisms associated with tissue fibrosis.* American Journal of Physiology-Cell Physiology, 2013. **304**(3): p. C216-C225.
14. Plikus, M.V., et al., *Fibroblasts: Origins, definitions, and functions in health and disease.* Cell, 2021. **184**(15): p. 3852-3872.
15. Reeds, P.J. and T.A. Davis, *Of flux and flooding: the advantages and problems of different isotopic methods for quantifying protein turnover in vivo: I. Methods based on the dilution of a tracer.* Current Opinion in Clinical Nutrition & Metabolic Care, 1999. **2**(1): p. 23-28.
16. Sala, A.J., L.C. Bott, and R.I. Morimoto, *Shaping proteostasis at the cellular, tissue, and organismal level.* J Cell Biol, 2017. **216**(5): p. 1231-1241.
17. Goodman, C.A. and T.A. Hornberger, *Measuring protein synthesis with SUnSET: a valid alternative to traditional techniques?* Exerc Sport Sci Rev, 2013. **41**(2): p. 107-15.
18. Schmidt, E.K., et al., *SUnSET, a nonradioactive method to monitor protein synthesis.* Nature Methods, 2009. **6**(4): p. 275-277.
19. Aviner, R., *The science of puromycin: From studies of ribosome function to applications in biotechnology.* Comput Struct Biotechnol J, 2020. **18**: p. 1074-1083.
20. Lee, J.M., et al., *Control of protein stability by post-translational modifications.* Nat Commun, 2023. **14**(1): p. 201.
21. Callis, J., *Regulation of Protein Degradation.* Plant Cell, 1995. **7**(7): p. 845-857.
22. Varshavsky, A., *Regulated protein degradation.* Trends in Biochemical Sciences, 2005. **30**(6): p. 283-286.
23. Barth, S., D. Glick, and K.F. Macleod, *Autophagy: assays and artifacts.* The Journal of Pathology, 2010. **221**(2): p. 117-124.
24. Glick, D., S. Barth, and K.F. Macleod, *Autophagy: cellular and molecular mechanisms.* The Journal of Pathology, 2010. **221**(1): p. 3-12.
25. Zhang, B., et al., *Mechanically induced autophagy is associated with ATP metabolism and cellular viability in osteocytes in vitro.* Redox Biol, 2018. **14**: p. 492-498.
26. Mizushima, N., *Autophagy: process and function.* Genes Dev, 2007. **21**(22): p. 2861-73.
27. Jain, A., et al., *p62/SQSTM1 Is a Target Gene for Transcription Factor NRF2 and Creates a Positive Feedback Loop by Inducing Antioxidant Response Element-driven Gene Transcription*.* Journal of Biological Chemistry, 2010. **285**(29): p. 22576-22591.

28. Burman, A., H. Tanjore, and T.S. Blackwell, *Endoplasmic reticulum stress in pulmonary fibrosis.* Matrix Biology, 2018. **68-69**: p. 355-365.

29. Hetz, C., K. Zhang, and R.J. Kaufman, *Mechanisms, regulation and functions of the unfolded protein response.* Nat Rev Mol Cell Biol, 2020. **21**(8): p. 421-438.

30. Frakes, A.E. and A. Dillin, *The UPRER: sensor and coordinator of organismal homeostasis.* Molecular cell, 2017. **66**(6): p. 761-771.

31. Wouters, B.G. and M. Koritzinsky, *Hypoxia signalling through mTOR and the unfolded protein response in cancer.* Nature Reviews Cancer, 2008. **8**(11): p. 851-864.

32. Liu, C.Y., M. Schröder, and R.J. Kaufman, *Ligand-independent dimerization activates the stress response kinases IRE1 and PERK in the lumen of the endoplasmic reticulum.* Journal of Biological Chemistry, 2000. **275**(32): p. 24881-24885.

33. Harding, H.P., et al., *Perk is essential for translational regulation and cell survival during the unfolded protein response.* Molecular cell, 2000. **5**(5): p. 897-904.

34. Oyadomari, S. and M. Mori, *Roles of CHOP/GADD153 in endoplasmic reticulum stress.* Cell Death & Differentiation, 2004. **11**(4): p. 381-389.

35. Hu, H., et al., *The C/EBP Homologous Protein (CHOP) Transcription Factor Functions in Endoplasmic Reticulum Stress-Induced Apoptosis and Microbial Infection.* Front Immunol, 2018. **9**: p. 3083.

36. Sasikumar, A.N., W.B. Perez, and T.G. Kinzy, *The many roles of the eukaryotic elongation factor 1 complex.* WIREs RNA, 2012. **3**(4): p. 543-555.

37. Roger, A.J., et al., *An evaluation of elongation factor 1 alpha as a phylogenetic marker for eukaryotes.* Molecular Biology and Evolution, 1999. **16**(2): p. 218-233.

38. Negrutskii, B.S. and A.V. El'skaya, *Eukaryotic Translation Elongation Factor 1α: Structure, Expression, Functions, and Possible Role in Aminoacyl-tRNA Channeling*, in *Progress in Nucleic Acid Research and Molecular Biology*, K. Moldave, Editor. 1998, Academic Press. p. 47-78.

39. Mateyak, M.K. and T.G. Kinzy, *eEF1A: thinking outside the ribosome.* J Biol Chem, 2010. **285**(28): p. 21209-13.

40. Cristiano, L., *The pseudogenes of eukaryotic translation elongation factors (EEFs): Role in cancer and other human diseases.* Genes Dis, 2022. **9**(4): p. 941-958.

41. Chan, J.J. and Y. Tay, *Noncoding RNA: RNA regulatory networks in cancer.* International journal of molecular sciences, 2018. **19**(5): p. 1310.

42. Poliseno, L., A. Marranci, and P.P. Pandolfi, *Pseudogenes in human cancer.* Frontiers in medicine, 2015. **2**: p. 68.

43. Poliseno, L., *Pseudogenes: newly discovered players in human cancer.* Science signaling, 2012. **5**(242): p. re5-re5.

44. Lund, A., et al., *Assignment of Human Elongation Factor 1α Genes: EEF1AMaps to Chromosome 6q14 andEEF1A2to 20q13. 3.* Genomics, 1996. **36**(2): p. 359-361.

45. Madsen, H.O., et al., *Retropseudogenes constitute the major part of the human elongation factor 1α gene family.* Nucleic acids research, 1990. **18**(6): p. 1513-1516.

46. Johnsson, P., K.V. Morris, and D. Grandér, *Pseudogenes: a novel source of trans-acting antisense RNAs.* Pseudogenes: Functions and Protocols, 2014: p. 213-226.

47. Pei, B., et al., *The GENCODE pseudogene resource.* Genome biology, 2012. **13**: p. 1-26.

48. McDonell, L. and G. Drouin, *The abundance of processed pseudogenes derived from glycolytic genes is correlated with their expression level.* Genome, 2012. **55**(2): p. 147-151.

49. Khacho, M., et al., *eEF1A is a novel component of the mammalian nuclear protein export machinery.* Molecular Biology of the Cell, 2008. **19**(12): p. 5296-5308.

50. Li, L., et al., *Expanded polyalanine tracts function as nuclear export signals and promote protein mislocalization via eEF1A1 factor.* Journal of Biological Chemistry, 2017. **292**(14): p. 5784-5800.

51. Francisco, C., *Role of eEF1A in the Nuclear Export of the VHL Tumour Suppressor Protein*. 2012: University of Ottawa (Canada).

52. Lin, C.-Y., et al., *Contradictory mRNA and protein misexpression of EEF1A1 in ductal breast carcinoma due to cell cycle regulation and cellular stress.* Scientific Reports, 2018. **8**(1): p. 13904.

53. Yang, F., et al., *Identification of an actin-binding protein from Dictyostelium as elongation factor 1a.* Nature, 1990. **347**(6292): p. 494-496.

54. Snape, N., et al., *The eukaryotic translation elongation factor 1A regulation of actin stress fibers is important for infectious RSV production.* Virology Journal, 2018. **15**(1): p. 182.

55. Liu, G., et al., *F-actin sequesters elongation factor 1alpha from interaction with aminoacyl-tRNA in a pH-dependent reaction.* J Cell Biol, 1996. **135**(4): p. 953-63.

56. Stoianov, A.M., et al., *Elongation Factor 1A-1 Is a Mediator of Hepatocyte Lipotoxicity Partly through Its Canonical Function in Protein Synthesis.* PLOS ONE, 2015. **10**(6): p. e0131269.

57. Kis, K., X. Liu, and J.S. Hagood, *Myofibroblast differentiation and survival in fibrotic disease.* Expert reviews in molecular medicine, 2011. **13**: p. e27.

58. Tallquist, M.D., *Cardiac Fibroblast Diversity.* Annual Review of Physiology, 2020. **82**(1): p. 63-78.

59. Reed, J.C., *Mechanisms of apoptosis.* The American journal of pathology, 2000. **157**(5): p. 1415-1430.

60. Mingot, J.M., et al., *eEF1A mediates the nuclear export of SNAG-containing proteins via the Exportin5-aminoacyl-tRNA complex.* Cell Rep, 2013. **5**(3): p. 727-37.

61. Dapas, B., et al., *Effects of eEF1A1 targeting by aptamer/siRNA in chronic lymphocytic leukaemia cells.* International Journal of Pharmaceutics, 2020. **574**: p. 118895.

62. Grund, A., et al., *TIP30 counteracts cardiac hypertrophy and failure by inhibiting translational elongation.* EMBO Mol Med, 2019. **11**(10): p. e10018.

63. White, K.M., et al., *Plitidepsin has potent preclinical efficacy against SARS-CoV-2 by targeting the host protein eEF1A.* Science, 2021. **371**(6532): p. 926-931.

64. Roux, P.P. and I. Topisirovic, *Regulation of mRNA translation by signaling pathways.* Cold Spring Harbor perspectives in biology, 2012. **4**(11): p. a012252.

65. Vislovukh, A.A., et al., *mRNAs coding for A1 and A2 isoforms of translation factor eEF1A demonstrate different half-lives while A1 and A2 proteins are similarly stable in MCF7 cells.* Biopolymers and cell, 2013(29,№ 5): p. 389-394.

66. Baird, T.D. and R.C. Wek, *Eukaryotic initiation factor 2 phosphorylation and translational control in metabolism.* Advances in nutrition, 2012. **3**(3): p. 307-321.

67. Jackson, R.J., C.U. Hellen, and T.V. Pestova, *The mechanism of eukaryotic translation initiation and principles of its regulation.* Nature reviews Molecular cell biology, 2010. **11**(2): p. 113-127.

68. Perez, W.B. and T.G. Kinzy, *Translation Elongation Factor 1A Mutants with Altered Actin Bundling Activity Show Reduced Aminoacyl-tRNA Binding and Alter Initiation via eIF2α Phosphorylation *.* Journal of Biological Chemistry, 2014. **289**(30): p. 20928-20938.

69. Shcherbakov, D., et al., *Ribosomal mistranslation leads to silencing of the unfolded protein response and increased mitochondrial biogenesis.* Communications Biology, 2019. **2**(1): p. 381.

70. Shin, J.-H. and S.-H. Min, *Novel functional roles of caspase-related genes in the regulation of apoptosis and autophagy.* The Korean Journal of Physiology & Pharmacology: Official Journal of the Korean Physiological Society and the Korean Society of Pharmacology, 2016. **20**(6): p. 573.

71. Tanida, I., T. Ueno, and E. Kominami, *LC3 and Autophagy.* Methods Mol Biol, 2008. **445**: p. 77-88.

72. Prommahom, A. and P. Dharmasaroja, *Effects of eEF1A2 knockdown on autophagy in an MPP+-induced cellular model of Parkinson's disease.* Neuroscience Research, 2021. **164**: p. 55-69.

73. Khwanraj, K., et al., *Comparative mRNA expression of eEF1A isoforms and a PI3K/Akt/mTOR pathway in a cellular model of Parkinson's disease.* Parkinson's Disease, 2016. **2016**.

74. Bosutti, A., et al., *High eEF1A1 Protein Levels Mark Aggressive Prostate Cancers and the In Vitro Targeting of eEF1A1 Reveals the eEF1A1–actin Complex as a New Potential Target for Therapy.* International Journal of Molecular Sciences, 2022. **23**(8): p. 4143.

75. Liu, Y., et al., *MLIF Modulates Microglia Polarization in Ischemic Stroke by Targeting eEF1A1.* Front Pharmacol, 2021. **12**: p. 725268.

76. George, G., et al., *Gene co-expression network analysis for identifying genetic markers in Parkinson's disease - a three-way comparative approach.* Genomics, 2019. **111**(4): p. 819-830.

77. Rubinsztein, D.C., et al., *Autophagy and Its Possible Roles in Nervous System Diseases, Damage and Repair.* Autophagy, 2005. **1**(1): p. 11-22.

78. Huang, Q., et al., *Akt2 kinase suppresses glyceraldehyde-3-phosphate dehydrogenase (GAPDH)-mediated apoptosis in ovarian cancer cells via phosphorylating GAPDH at threonine 237 and decreasing its nuclear translocation.* Journal of Biological Chemistry, 2011. **286**(49): p. 42211-42220.

79. Cavallius, J., S.I.S. Rattan, and B.F.C. Clark, *Changes in activity and amount of active elongation factor 1α in aging and immortal human fibroblast cultures.* Experimental Gerontology, 1986. **21**(3): p. 149-157.

80. Grassi, G., et al., *The expression levels of the translational factors eEF1A 1/2 correlate with cell growth but not apoptosis in hepatocellular carcinoma cell lines with different differentiation grade.* Biochimie, 2007. **89**(12): p. 1544-1552.

81. Gangwani, L., et al., *Interaction of ZPR1 with translation elongation factor-1α in proliferating cells.* The Journal of cell biology, 1998. **143**(6): p. 1471-1484.

82. Kanellakis, P., et al., *A pro-fibrotic role for interleukin-4 in cardiac pressure overload.* Cardiovascular Research, 2012. **95**(1): p. 77-85.

83. Leask, A., *Potential therapeutic targets for cardiac fibrosis: TGFβ, angiotensin, endothelin, CCN2, and PDGF, partners in fibroblast activation.* Circulation research, 2010. **106**(11): p. 1675-1680.

84. Pinzani, M., *Pathophysiology of liver fibrosis.* Digestive diseases, 2015. **33**(4): p. 492-497.

85. Sferra, R., et al., *Expression of pro-fibrotic and anti-fibrotic molecules in dimethylnitrosamine-induced hepatic fibrosis.* Pathology - Research and Practice, 2017. **213**(1): p. 58-65.

86. Inagaki, Y. and I. Okazaki, *Emerging insights into transforming growth factor β Smad signal in hepatic fibrogenesis.* Gut, 2007. **56**(2): p. 284-292.

87. Ma, Z.G., et al., *Cardiac fibrosis: new insights into the pathogenesis.* Int J Biol Sci, 2018. **14**(12): p. 1645-1657.

88. Frieler, R.A. and R.M. Mortensen, *Immune cell and other noncardiomyocyte regulation of cardiac hypertrophy and remodeling.* Circulation, 2015. **131**(11): p. 1019-1030.

89. Rosenbloom, J., F.A. Mendoza, and S.A. Jimenez, *Strategies for anti-fibrotic therapies.* Biochimica et Biophysica Acta (BBA) - Molecular Basis of Disease, 2013. **1832**(7): p. 1088-1103.

90. Inagaki, Y., R. Higashiyama, and K. Higashi, *Novel anti-fibrotic modalities for liver fibrosis: molecular targeting and regenerative medicine in fibrosis therapy.* Journal of gastroenterology and hepatology, 2012. **27**: p. 85-88.

91. McVicker, B.L. and R.G. Bennett, *Novel anti-fibrotic therapies.* Frontiers in pharmacology, 2017. **8**: p. 318.

92. Trusina, A. and C. Tang, *The unfolded protein response and translation attenuation: a modelling approach.* Diabetes, Obesity and Metabolism, 2010. **12**(s2): p. 27-31.

93. Marciniak, S.J. and D. Ron, *Endoplasmic reticulum stress signaling in disease.* Physiological reviews, 2006. **86**(4): p. 1133-1149.

94. Harding, H.P., Y. Zhang, and D. Ron, *Protein translation and folding are coupled by an endoplasmic-reticulum-resident kinase.* Nature, 1999. **397**(6716): p. 271-274.

95. Vera, M., et al., *The translation elongation factor eEF1A1 couples transcription to translation during heat shock response.* eLife, 2014. **3**: p. e03164.

96. Rayaprolu, S., et al., *Cell type-specific biotin labeling in vivo resolves regional neuronal and astrocyte proteomic differences in mouse brain.* Nature Communications, 2022. **13**(1): p. 2927.

97. Wilson, R.B., et al., *The marine compound and elongation factor 1A1 inhibitor, didemnin B, provides benefit in western diet-induced non-alcoholic fatty liver disease.* Pharmacological Research, 2020. **161**: p. 105208.

98. Chun, H.G., et al., *Didemnin B. The first marine compound entering clinical trials as an antineoplastic agent.* Invest New Drugs, 1986. **4**(3): p. 279-84.

99. Branon, T.C., et al., *Efficient proximity labeling in living cells and organisms with TurboID.* Nature biotechnology, 2018. **36**(9): p. 880-887.

100. Hetherington, A., et al., *Treatment with didemnin B, an elongation factor 1A inhibitor, improves hepatic lipotoxicity in obese mice.* Physiological reports, 2016. **4**.